

DC Arc Flash on Photovoltaic Equipment

2018 TECHNICAL REPORT

DC Arc Flash on Photovoltaic Equipment

EPRI Project Manager
T. Short



3420 Hillview Avenue
Palo Alto, CA 94304-1338
USA

PO Box 10412
Palo Alto, CA 94303-0813
USA

800.313.3774
650.855.2121

askpri@epri.com

www.epri.com

3002014124

Final Report, June 2018

DISCLAIMER OF WARRANTIES AND LIMITATION OF LIABILITIES

THIS DOCUMENT WAS PREPARED BY THE ORGANIZATION NAMED BELOW AS AN ACCOUNT OF WORK SPONSORED OR COSPONSORED BY THE ELECTRIC POWER RESEARCH INSTITUTE, INC. (EPRI). NEITHER EPRI, ANY MEMBER OF EPRI, ANY COSPONSOR, THE ORGANIZATION BELOW, NOR ANY PERSON ACTING ON BEHALF OF ANY OF THEM:

(A) MAKES ANY WARRANTY OR REPRESENTATION WHATSOEVER, EXPRESS OR IMPLIED, (I) WITH RESPECT TO THE USE OF ANY INFORMATION, APPARATUS, METHOD, PROCESS, OR SIMILAR ITEM DISCLOSED IN THIS DOCUMENT, INCLUDING MERCHANTABILITY AND FITNESS FOR A PARTICULAR PURPOSE, OR (II) THAT SUCH USE DOES NOT INFRINGE ON OR INTERFERE WITH PRIVATELY OWNED RIGHTS, INCLUDING ANY PARTY'S INTELLECTUAL PROPERTY, OR (III) THAT THIS DOCUMENT IS SUITABLE TO ANY PARTICULAR USER'S CIRCUMSTANCE; OR

(B) ASSUMES RESPONSIBILITY FOR ANY DAMAGES OR OTHER LIABILITY WHATSOEVER (INCLUDING ANY CONSEQUENTIAL DAMAGES, EVEN IF EPRI OR ANY EPRI REPRESENTATIVE HAS BEEN ADVISED OF THE POSSIBILITY OF SUCH DAMAGES) RESULTING FROM YOUR SELECTION OR USE OF THIS DOCUMENT OR ANY INFORMATION, APPARATUS, METHOD, PROCESS, OR SIMILAR ITEM DISCLOSED IN THIS DOCUMENT.

REFERENCE HEREIN TO ANY SPECIFIC COMMERCIAL PRODUCT, PROCESS, OR SERVICE BY ITS TRADE NAME, TRADEMARK, MANUFACTURER, OR OTHERWISE, DOES NOT NECESSARILY CONSTITUTE OR IMPLY ITS ENDORSEMENT, RECOMMENDATION, OR FAVORING BY EPRI.

THE ELECTRIC POWER RESEARCH INSTITUTE (EPRI) PREPARED THIS REPORT.

NOTE

For further information about EPRI, call the EPRI Customer Assistance Center at 800.313.3774 or e-mail askepri@epri.com.

Electric Power Research Institute, EPRI, and TOGETHER...SHAPING THE FUTURE OF ELECTRICITY are registered service marks of the Electric Power Research Institute, Inc.

Copyright © 2018 Electric Power Research Institute, Inc. All rights reserved.



Acknowledgments

The Electric Power Research Institute (EPRI) prepared this report.

Principal Investigators

T. Short

J. Potvin

B. Paudyal

This report describes research sponsored by EPRI. EPRI would like to acknowledge the support of the following organizations and individuals: Justin Woodard of National Grid was instrumental in designing, setting up, and running tests, and in overall project management. Glenn McGillicuddy and Jonathan Salsman of Industria Engineering led the site preparations and design and construction of test fixtures.

This publication is a corporate document that should be cited in the literature in the following manner:

*DC Arc Flash on Photovoltaic
Equipment.*

EPRI, Palo Alto, CA: 2018.
3002014124.



Abstract

Protection from arc flash on ac systems is relatively well understood. Calculation approaches have been applied across many equipment types and voltages in many industries. These approaches are backed by a wide range of industry tests. Arc flash on dc systems such as photovoltaic systems is relatively unknown. Several calculation approaches have been proposed, but these have not been backed by any industry tests on equipment.

This report provides an overview of arc-flash hazard in terms of incident energy and arc-flash energy on photovoltaic equipment. The experiment site is a utility-owned ground-mount photovoltaic plant with a 1-MWdc nameplate capacity located at Sturbridge, MA.

Three equipment arrangements were tested: a 20 × 20 × 20-in. (51 × 51 × 51-cm) box, a combiner box, and a mocked-up inverter cabinet. The results from the box testing helped to establish the characteristics of the dc source and to allow comparison to industry-standard ac testing. The results from the combiner box and inverter cabinet provided real-world results. The results were also compared with industry models of dc arc flash, and a new model was developed based on the test results.

Keywords

Arc flash
Direct current (dc)
Photovoltaics (PV)
Safety

Deliverable Number: 3002014124

Product Type: Technical Report

Product Title: DC Arc Flash on Photovoltaic Equipment

PRIMARY AUDIENCE: Solar photovoltaic (PV) plant designers, owners, and operators

SECONDARY AUDIENCE: Solar PV equipment manufacturers and safety and standards organizations

KEY RESEARCH QUESTION

The rapid release of thermal energy, pressure waves, and electromagnetic interference emanating from an arc flash all pose risks to people and equipment in a PV plant. The existing calculation methods for incident energy of a dc arc flash contradict one another and are rooted in theory, not actual physical testing. The incident energy calculation dictates the level of personal protective equipment (PPE) that field workers are required to wear when servicing fielded equipment. Overly burdensome PPE may decrease dexterity and lead to an accident; inadequate PPE also comes with safety risks.

RESEARCH OVERVIEW

This report provides an overview of dc arc-flash hazards in terms of incident energy. The experiments were performed on a ground-mounted PV plant with a 1-MWdc nameplate capacity located at Sturbridge, MA. Arc-flash experiments were performed on the following PV equipment: a combiner box, an inverter, and a box setup (a 20 x 20 x 20-in [51 x 51 x 51-cm] metal cube). Behavior of the arc, including current, voltage, and power were evaluated for different equipment conditions and different PV array connections. Incident energies were measured, and these were compared to common, theory-based calculation models.

KEY FINDINGS

- Incident energy exposures to workers are modest, assuming that a worker can self-extract in a reasonable time (2 seconds for example). All incident energy measurements at a distance of 18 in. (46 cm) to the equipment electrodes were less than 3.6 cal/cm². Extrapolating all tests to the highest irradiance and to a 2-second duration produces a maximum adjusted incident energy of 5.2 cal/cm². Daily wear clothing of 8 cal/cm² should be sufficient for most equipment and PV array sizes (see Section 3).
- The nonlinear characteristics of PV panels are important to include. The PV array acts as a constant-current supply with currents near the short-circuit portion of the current-voltage characteristic curve (I-V curve) of the array. The median arc voltage in tests was 234 V, which was approximately 30% of the open-circuit voltage (see Section 3).
- The measured incident energies are lower than those of most of the industry models. Two of the industry models predicted more than five times the energies measured. These “maximum power” methods overpredicted energies. One industry model provided results that were reasonable for an electrode gap of 0.5 in. (1.3 cm). For a gap of 2 in. (5 cm), this model overpredicted incident energies by a factor of two. None of the models adequately predicted incident energies across gap sizes. None of the models adequately predicted arc currents and arc voltages (see Section 4).
- A custom model was developed to estimate incident energies on PV systems. The model predicts incident energy as a linear function of the short-circuit current of the array and the fault duration (see Section 4).

- Incident energies were comparable to those of ac arc flash when comparing normalized arc energies (see Section 3).
- Arcs sustained in many of the tests, and arcs also self-cleared in some tests. The open-circuit dc bus voltage was nominally 1000 V. During tests, the open-circuit array voltage was approximately 750 V. This voltage sustained arcs between gaps as long as 10 in. (25 cm). With longer gaps, arcs were more likely to self-clear. None of the arcs self-cleared in the combiner box, in which the gaps between electrodes were less than 2 in. (5 cm) (see Section 3).
- If the inverter was on, there was minimal feed from the inverter to the arc. The main source of energy is still the PV array (see Section 3).
- The grounding and connection of the negative terminal is an important consideration. If the negative terminal is floating, an arc is less likely to sustain because the equipment case cannot act as a return path for the current. This is particularly important in the inverter cabinet (see Section 3).

WHY THIS MATTERS

Protection from arc flash on ac systems is relatively well understood. Calculation approaches have been applied across many equipment types and voltages in many industries. These approaches are backed by a wide range of industry tests. Arc flash on dc systems such as PV systems is relatively unknown. Several calculation approaches have been proposed, but these have not been backed by any industry tests on equipment. Understanding and improving such calculations will allow plant workers to be better protected.

HOW TO APPLY RESULTS

PV plant owners and operators can use these results to design equipment labels and to implement programs to protect maintenance workers. Protection against maximum expected incident energies can be based on adjusted test results or based on the model provided.

LEARNING AND ENGAGEMENT OPPORTUNITIES

EPRI is continuing testing and modeling on dc arc flash in photovoltaic equipment as part of a cooperative agreement with the U.S. Department of Energy. This work will focus particularly on 1500-V dc systems.

EPRI CONTACTS: Tom Short, Senior Technical Executive, tshort@epri.com

PROGRAM: Distribution Systems, 180

Together...Shaping the Future of Electricity®

Electric Power Research Institute

3420 Hillview Avenue, Palo Alto, California 94304-1338 • PO Box 10412, Palo Alto, California 94303-0813 USA

800.313.3774 • 650.855.2121 • askepri@epri.com • www.epri.com

© 2018 Electric Power Research Institute (EPRI), Inc. All rights reserved. Electric Power Research Institute, EPRI, and TOGETHER...SHAPING THE FUTURE OF ELECTRICITY are registered service marks of the Electric Power Research Institute, Inc.

Table of Contents

Abstract.....	v
Executive Summary	vii
Section 1: Introduction	1-1
Section 2: Experiment Setup and Tests.....	2-1
20-in Box	2-4
Combiner Box	2-9
Inverter Cabinet	2-16
Results Summary	2-21
Section 3: Analysis of Results	3-1
Arc Current and Voltages.....	3-1
Incident Energies and Arc Energies	3-3
Arc-Flash Duration Versus Arc Energy	3-6
Impact of the PV Source	3-7
Effect of the Inverter Contribution	3-9
Directionality of the Arc Flash	3-10
Arc Stability and the Effect of Enclosure Grounding.....	3-12
Using Test Results to Determine Appropriate Protective Levels	3-14
Section 4: Models of Arc Flash in PV Systems	4-1
Industry Models	4-1
New Model Based on Tests	4-5
Section 5: Summary and Future Work	5-1
Key Findings.....	5-1
Future Work	5-2
Section 6: References	6-1

List of Figures

Figure 2-1 Single line diagram of the approximately 1-MWdc block feeding the test setups	2-2
Figure 2-2 Setup showing the dc contactor and switches for controlling source characteristics	2-3
Figure 2-3 Multi-sensor calorimeter array.....	2-4
Figure 2-4 Schematic and image of a box for arc-flash test... 2-5	
Figure 2-5 Arc initiation wire in place prior to test 1	2-6
Figure 2-6 Video frames from test 3	2-7
Figure 2-7 Electrodes after test 3	2-8
Figure 2-8 Schematic and image of a ARCCOM combiner box; showing the terminal points as the electrodes for an arc-flash event.....	2-9
Figure 2-9 Arc initiation in the combiner box for test 26.....	2-10
Figure 2-10 Video frames for test 26 with synced infrared video frames.....	2-10
Figure 2-11 Arc damage in the combiner box from test 26	2-11
Figure 2-12 Arc initiation in the combiner box for test 27... 2-12	
Figure 2-13 Video frames from test 28.....	2-13
Figure 2-14 Current and voltage waveforms for test 28	2-14
Figure 2-15 Damage from test 28	2-15
Figure 2-16 Image of an inverter cabinet used as a reference and the mocked-up assembly.....	2-16
Figure 2-17 Arc initiation in the inverter cabinet for test 21	2-18
Figure 2-18 Arc initiation in the inverter cabinet for test 22	2-18

Figure 2-19 Arc initiation in the inverter cabinet for test 23	2-19
Figure 2-20 Arc damage from test 23	2-19
Figure 2-21 Arc initiation in the inverter cabinet for test 25	2-19
Figure 2-22 Bus arrangement for test 29	2-20
Figure 2-23 Arc damage for test 29	2-20
Figure 2-24 Inverter before and during test 29	2-21
Figure 3-1 Arc current and voltage of a PV-array (1000 kW), 950 W/m ² irradiances and 53oC PV-module temperature	3-1
Figure 3-2 Ratios of V _{arc} /V _{mp} and I _{arc} /I _{mp}	3-2
Figure 3-3 Incident and arc-flash energy as the function of PV array size	3-3
Figure 3-4 Arc energy (MJ) versus incident energy (cal/cm ²) for all three experimental setups.....	3-4
Figure 3-5 Arc energy (MJ) versus incident energy (cal/cm ²) for the 20-in box setup.....	3-5
Figure 3-6 Comparison of energy transfers for ac and dc tests	3-6
Figure 3-7 Measured arc-flash energy vs arc duration	3-6
Figure 3-8 Arc current and voltage of a PV-array (1000kW), 950 Wm ⁻² irradiances and 53oC PV-module temperature	3-7
Figure 3-9 Power-Voltage characteristic of PV-array (~1000 kW, 950 W/m ² , 53oC module temperature). ..	3-8
Figure 3-10 Average current and voltage during arc-flash with the inverter on.....	3-9
Figure 3-11 Arc flash and arc movement during test #34 in the 20-in (51-cm) box.....	3-10
Figure 3-12 Arc flash and arc movement during a test #28 in the combiner box.....	3-11
Figure 3-13 Arc flash and arc movement during a test #29 in the inverter assembly	3-11

Figure 3-14 Arc voltage and current in test 21 that self-extinguished.....	3-12
Figure 3-15 Infrared filtered video frames for test 30	3-13
Figure 3-16 Histogram of adjusted incident energies	3-14
Figure 3-17 Cumulative distribution of adjusted incident energies.....	3-15

List of Tables

Table 2-1 Variables for (20x20x20-in) box-experiment	2-5
Table 2-2 Variables for the combiner box experiments.....	2-9
Table 2-3 Variables for inverter-cabinet experiments.....	2-17
Table 2-4 Summary of test results.....	2-22
Table 3-1 Summary of results for the box experiments.....	3-4
Table 3-2 Arc current, voltage, and power (I_{arc} , V_{arc} , and P_{arc}) of a PV-array during an arc flash in a PV inverter test (Test #27).....	3-7
Table 3-3 P_{arc}/P_{max} for different test fixtures showing arc gap and connected array source size	3-8
Table 3-4 Total and spike (due to the inverter) arc current, voltage, and energy of two experiments	3-10
Table 3-5 Adjusted incident energies	3-16
Table 4-1 Measured incident energy and calculated incident energies using different models.....	4-2
Table 4-2 Measured arc voltage and calculated arc voltages using different models	4-3
Table 4-3 Measured arc current and calculated arc currents using different models.....	4-4
Table 4-4 Comparison of measurements to predictions from the empirical model	4-7



Section 1: Introduction

Protection from arc-flash on ac systems is relatively well understood. Calculation approaches have been applied across many equipment types and voltages in many industries. These are backed by a wide range of industry tests. The main industry calculation approach, IEEE 1584-2002 [1], covers only ac systems. The National Electrical Safety Code [2] addresses low-voltage ac arc flash, but it does not cover dc arc flash. The NFPA 70E [3] covers ac and dc arc flash, and the work of Doan [4] is cited in an informative annex.

EPRI has tested arc flash in many types of medium-voltage and low-voltage equipment ac equipment (EPRI 1018693 [5], EPRI 1022002 [6], EPRI 3002006373 [7], and EPRI 3002005598 [8]). These tests have shown that arc flash depends highly on equipment characteristics. This includes box effects and electrode characteristics. For low-voltage ac arc flash, the equipment characteristics can determine whether arcs self-sustain or whether they self-extinguish. It is unknown if that happens with a dc arc.

Arc-flash on dc systems such as photovoltaic (PV) systems is relatively unknown. Several calculation approaches have been proposed, but these have not been backed by any industry tests on equipment and contradict one another. The incident energy (IE) calculation dictates what level of personal protective equipment (PPE) field workers are required to wear when servicing fielded equipment. These also define the boundary distance from a potential arc-flash hazard. Overly burdensome PPE may reduce compliance, decrease dexterity, and increase accidents. Inadequate PPE also comes with obvious safety risks.

A series of staged tests on PV equipment driven by a PV source were performed in this work to better understand the hazards of dc arc-flash on photovoltaic equipment, namely inverter and combiner boxes. The main motive of this work is to measure the energy that worker could be subjected to near an arc. The work also addressed several research questions, including:

- For PV equipment, how conservative are existing dc calculation methods?
- How directional is the energy from an arc-flash in PV equipment? For ac arc-flash, in some equipment, the energy from the arc(s) is very directed. This can increase incident energies to workers.

- How do equipment geometries affect incident energies?
- How much do arcs move, and where to they move?
- How long do arcs become? Are they stable? Do they change over time during an event?
- What is the voltage across the arc? The arc voltage along with the current determine the power generated in the arc.

Experiments were performed to measure the incident energy (IE) of arc-flashes in PV equipment and study the current-voltage characteristic of the PV array during an arc-flash. The experiment site is a ground-mounted PV plant with a 2-MW_{dc} nameplate capacity in Sturbridge, MA. Tests were done on September 25th, and 26th, 2017, at various irradiance values ranging from 513 to 1000 W/m².



Section 2: Experiment Setup and Tests

Arc-flash experiments were designed to measure incident energies and arc-flash energy for three types of test fixtures: a test calibration box (20 in × 20 in × 20 in; 51 cm × 51 cm × 51 cm), a combiner box, and a mock inverter cabinet. Incident energy was measured using slug calorimeters based on ASTM 1959 [9] positioned at 18 in (46 cm) from the arc-initiation point. The calorimeter array also included sensors designed to measure the various components of incident energy [10].

The system consists of an array of approximately 1 MW_{dc} with 171 parallel strings of PV modules. Each string has 19 multi-crystalline silicon PV modules (in series) with a nameplate capacity of 305 W_{dc}. The 171 parallel strings are roughly divided in half (86 and 85) and connected into two separate dc buses that feed two separate 500-kW_{dc} inverters.

A single-line diagram of each bus and arc-flash test location is shown in Figure 2-1. See Appendix A for a more complete diagram. The following equipment was used to operate the tests and to capture results:

- Switch setup to control grounding and the source supply
- DC contactor with timing relay
- Fluke i1010 AC/DC current clamps
- Fluke 435 series II power quality and energy analyzer
- EPRI custom data acquisition system with slow channels for temperature and high-speed channels for voltage and current capture
- EPRI multi-sensor array with calorimeters
- Video cameras
- Seaward Solar Survey 200R incident energy meter

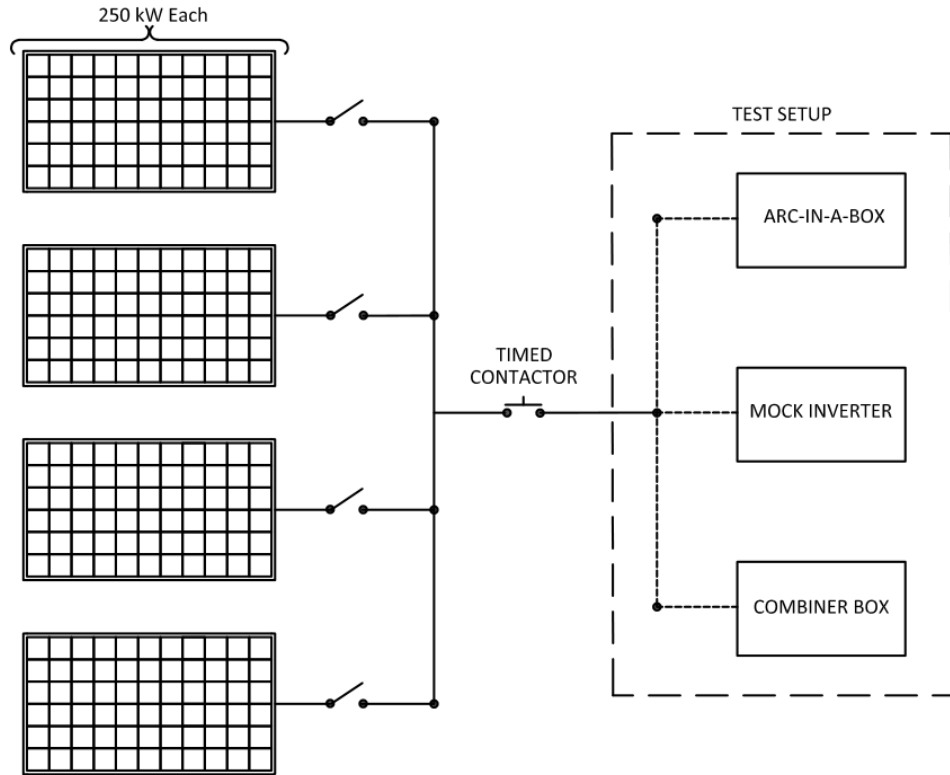


Figure 2-1
Single line diagram of the approximately 1-MW_{dc} block feeding the test setups

See Figure 2-2 for the switch setup along with some of the instrumentation. In this picture, the source is fed from the right, and the test fixtures are supplied by cables that leave on the left. The four switches on the right (marked in red) controlled how many array sources are connected to the test circuit. Each switch was fed by 250 kW of PV array. This is the positive terminal, and each switch was fed by two 2/0 Cu cables coming from the site inverters. The array sources were combined on a 3/8×3-in (1×7.6-cm) Cu busbar at the bottom of these four switches. From there, the combined array source connected to a dc contactor. From the dc contactor, two 4/0 Cu cables supplied the positive terminal to the test fixtures.

The negative terminals from the PV arrays are brought together on a 3/8×3-in (1×7.6-cm) Cu busbar, and two 4/0 Cu cables supplied the negative terminal to the test fixtures. One 4/0 Cu grounding cable was supplied to the test fixture. The cables supplying the test fixture could be moved between each of the three test fixtures.

In Figure 2-2, the “grounding switch” on the left side (marked with green) connected the positive and ground terminals as a safety measure. This switch was open during all tests. The second switch from the left (marked with white) controlled if the negative terminal was bonded. When this

switch was closed, the negative terminal was also tied to equipment cabinets and grounds. When this switch was open, the negative terminal was floating.

At the inverter, there was a connection between the negative terminal and ground through a 5-A circuit breaker. This was disconnected during tests. In practice, this circuit breaker should operate to isolate equipment grounds from the negative terminal.

The tests were initiated by closing a dc contactor. The contactor had a relay that controlled the duration of the test. After the timing set in the relay elapsed, the dc contactor opened. The relay timing was not exact. Many of the tests had a desired delay of 2 secs, but the relay operated typically operated in about 1.87 secs. Although the absolute timing was off, the operation time was repeatable between tests.

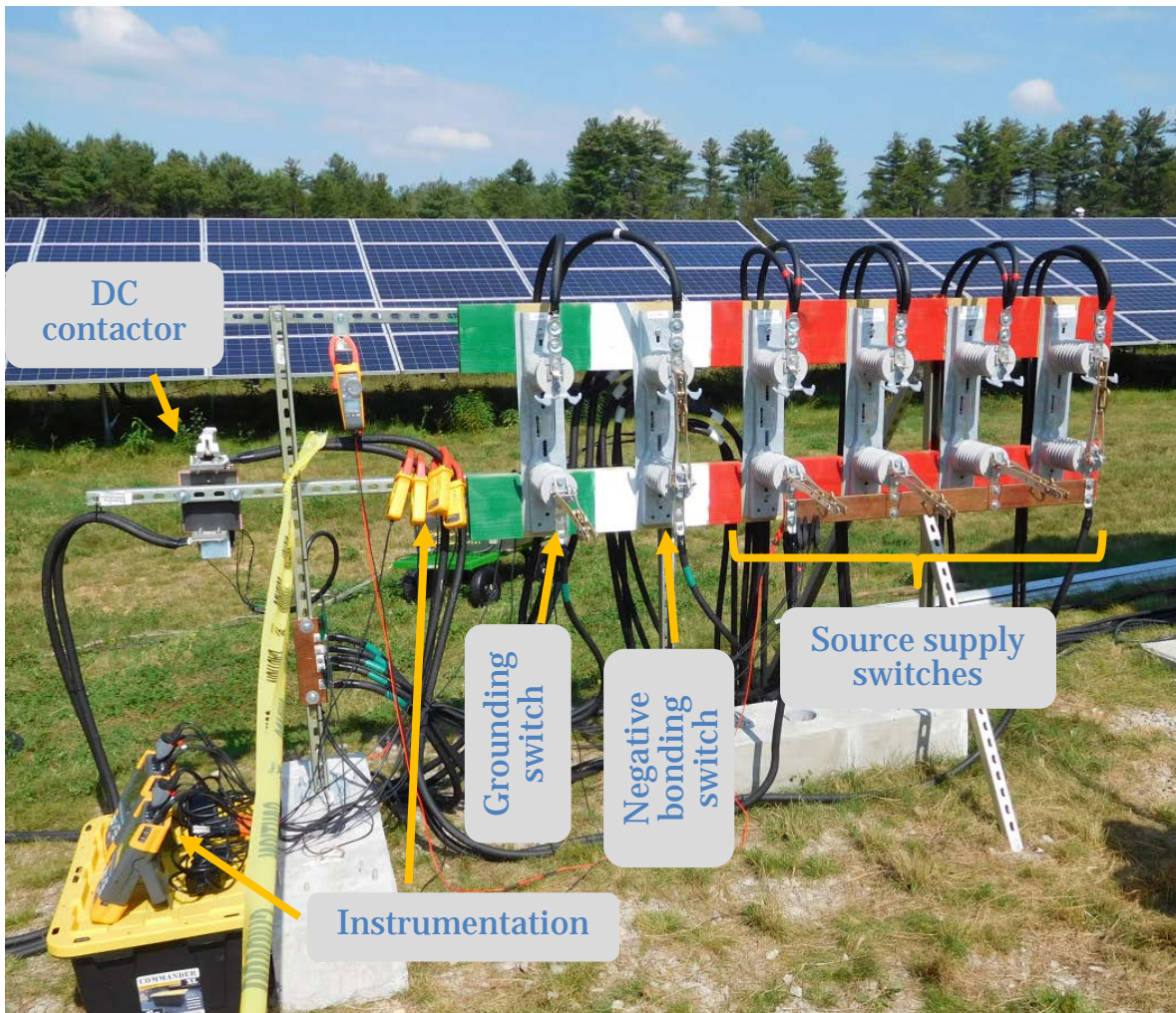


Figure 2-2
Setup showing the dc contactor and switches for controlling source characteristics

Figure 2-3 shows the calorimeter array used for tests. This includes several copper-slug calorimeters. These are copper disks with a thermocouple attached to the back. Instrumentation measured the temperature rise on the disks, and from that, the incident energy was measured. All incident energy measurements were taken at 18 in (46 cm) from the point where the arc was initiated.



Figure 2-3
Multi-sensor calorimeter array

Arc energy was calculated with measurements of arc current and arc voltage. Current was measured by using a Fluke i1010 ac/dc current clamp meter. High-speed cameras were also used to capture arc characteristics. Arc power was calculated by multiplying arc-current (I_{arc}) by arc voltage (V_{arc}). Details of test apparatus and assemblies are mentioned below.

20-in Box

There is a large body of industry data on ac arc flash in enclosed boxes. For these tests, a 20-inch (51-cm) cubic box was used. Ten arc-flash experiments were performed in this setup with four different PV-array sizes (dc name plate: 125, 250, 500, and 1000 kW) with a combination of different electrode spacings (0.5 and 2 in; 1.3 and 5 cm) and arc durations (0.5, 2, and 10 secs).

See Figure 2-4 for a schematic and image of the box. Table 2-1 shows the main input variables for the tests in the 20-in (51-cm) box, including PV array power (kW), electrode spacing, test duration, and inverter status (ON/OFF).

Faults were initiated by connecting the two electrodes with a 30-gauge copper wire (Figure 2-5). This wire vaporized quickly upon fault initiation. The circuit was opened by a dc contactor after a set time controlled by a timer.

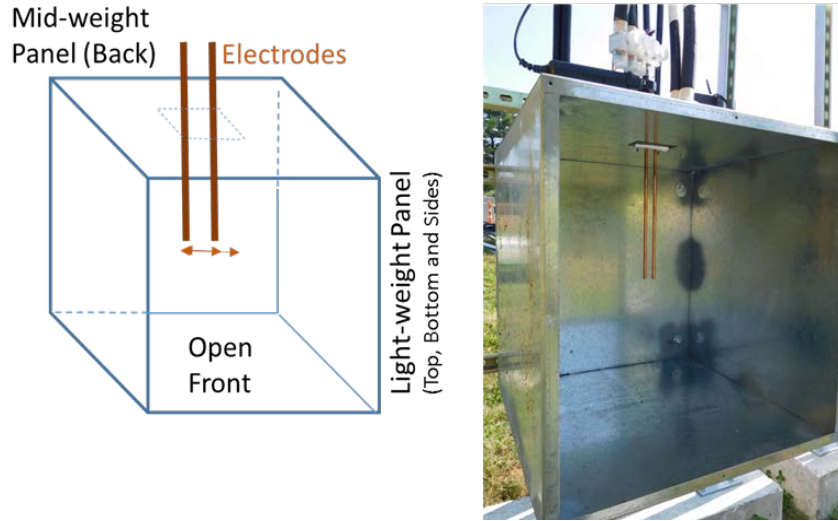


Figure 2-4
Schematic and image of a box for arc-flash test

Table 2-1
Variables for (20x20x20-in) box-experiment

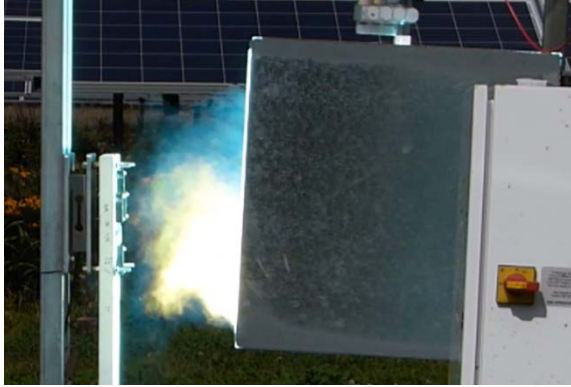
Experiment No.	PV Array dc Nameplate, (kW)	Electrode Spacing (in)	Target Duration (secs)	Negative Terminal Grounded(Y/N)	Inverter Status (Switch On/Off)
1	250	0.5	0.5	Y	OFF
2	250	0.5	0.5	Y	OFF
3	1000	0.5	2	Y	OFF
4	500	0.5	2	Y	ON
5	500	0.5	2	Y	OFF
6	1000	2	2	Y	OFF
7	1000	2	2	Y	OFF
34	1000	2	2	Y	OFF
35	1000	2	2	N	OFF
36	125	2	10	Y	OFF



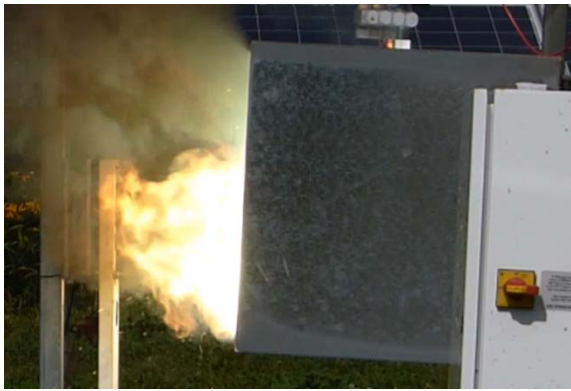
Figure 2-5
Arc initiation wire in place prior to test 1

Figure 2-6 shows video frames from test 3. This was the most energetic event. It had peak sun during tests with an incident energy of 1000 W/cm^2 . The maximum incident energy measured in this test was 3.6 cal/cm^2 . From three to four inches of the 0.25-in busbar eroded during this test (Figure 2-7).

0.1 secs



1.1 secs



Side view

Front view

Figure 2-6
Video frames from test 3



Figure 2-7
Electrodes after test 3

Combiner Box

Arc-flash experiments on an ARCCOM combiner box from Yaskawa Solectria Solar were performed with test variables as shown in Table 2-2. The schematic and image of a combiner box (open) are shown in Figure 2-8.

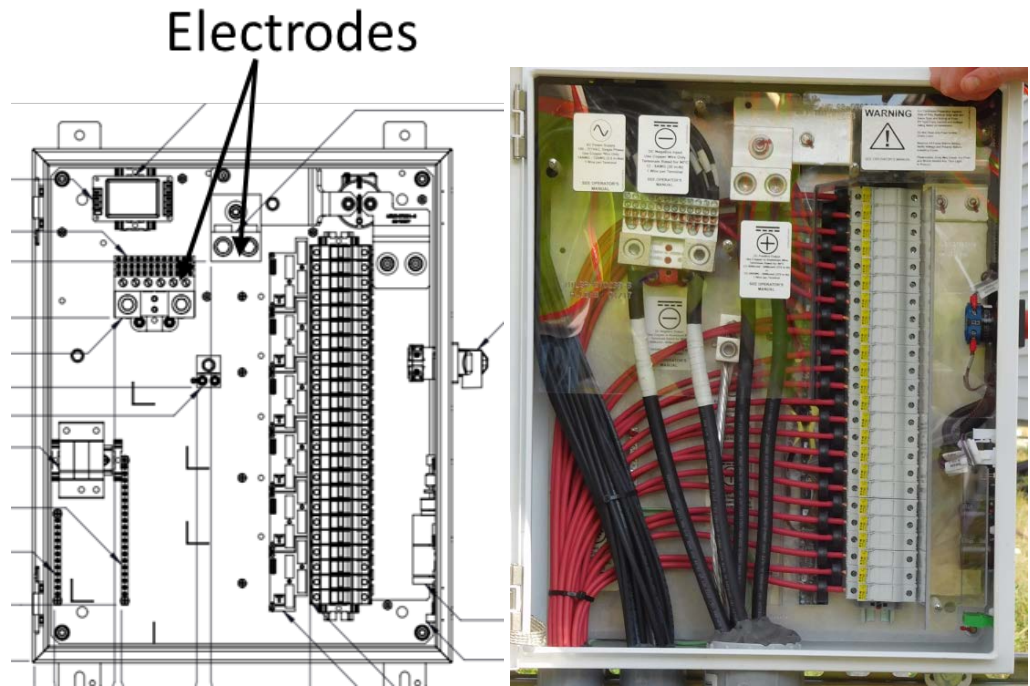


Figure 2-8
Schematic and image of an ARCCOM combiner box; showing the terminal points as the electrodes for an arc-flash event

Three arc-flash experiments were performed on the combiner box at 1000-kW PV-array size (dc name plate) for 2 and 10 secs of arc duration.

Table 2-2
Variables for the combiner box experiments

Experiment No.	PV-Array (dc-nameplate, kW)	Irradiance (W/m ²)	Target Duration (s)	Negative Terminal Grounded (Y/N)	Inverter Status (Switch On/Off)
26	1000	530	2	Y	OFF
27	1000	950	2	Y	OFF
28	1000	970	10	Y	OFF

In test 26, the fault was initiated with a short #30 Cu jumper wire from the positive terminal to the enclosure. As seen in Figure 2-9, the distances from this terminal to the metallic enclosure is less than one inch. See Figure 2-10 for video images from test 26 along with images from a video camera with an infrared-passing filter. The arc path started at the positive terminal, and it attached to the upper part of the box.

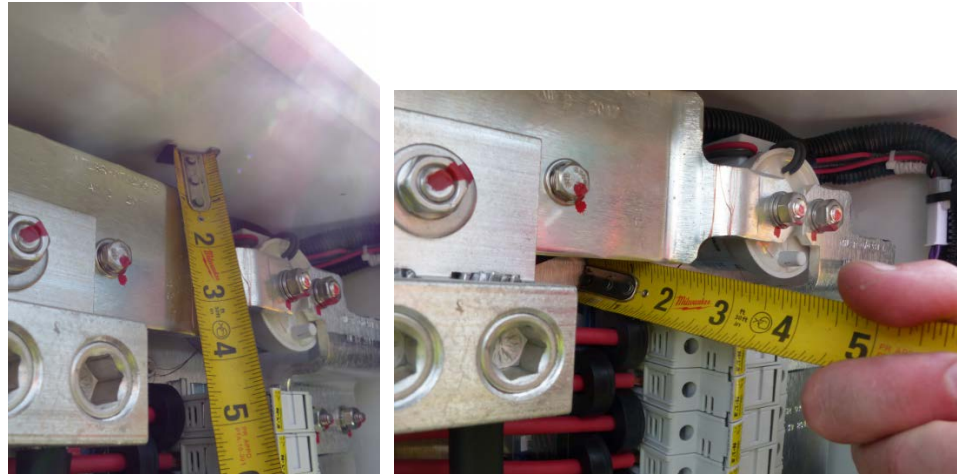
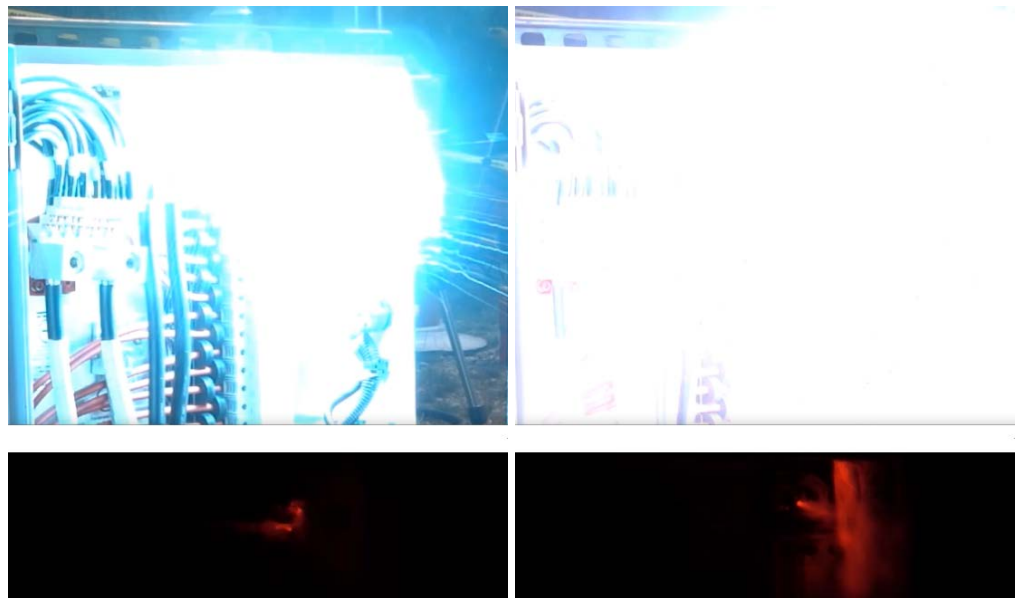


Figure 2-9
Arc initiation in the combiner box for test 26



Test start

0.2 secs

Figure 2-10
Video frames for test 26 with synced infrared video frames

Figure 2-11 shows the damage after this event. Arc damage occurred all along the bus on the right side of the cabinet.

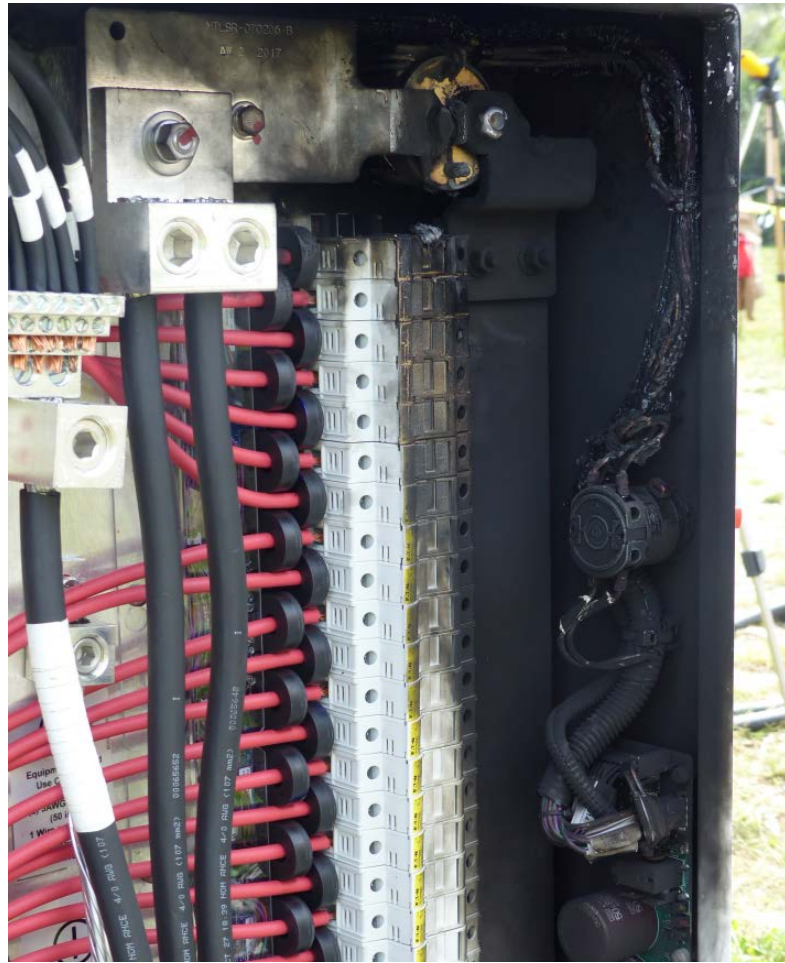


Figure 2-11
Arc damage in the combiner box from test 26

In test 27, the arc was initiated between the positive terminal and the negative terminal at the top of the enclosure. See Figure 2-12. The distance between these two terminals is approximately 0.5 in (1 cm).



*Figure 2-12
Arc initiation in the combiner box for test 27*

In test 28, the fault initiation was repeated for test 27, but the duration was extended to 10 secs.

During this test, the video showed that the output energy varied significantly during the test. See Figure 2-13. The reason for this is that the arc changed location and length. This caused the voltage to bounce from nearly shorted to over 700 V (about the open-circuit voltage). The arc self-cleared briefly during the event. Figure 2-14 shows the current and voltage during this test. During the event, a fuse operated in a combiner box in the array, and the current dropped accordingly.



Figure 2-13
Video frames from test 28

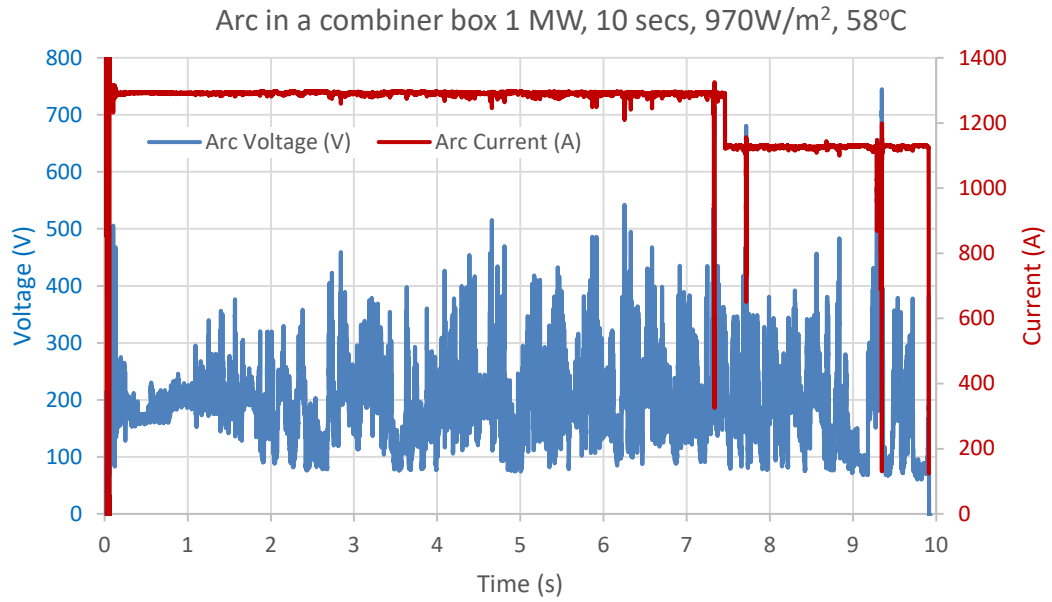


Figure 2-14
Current and voltage waveforms for test 28

The arcing mainly happened in the upper right part of the combiner box. The fault burned holes in the enclosure and burnt up some components inside (Figure 2-15).



*Figure 2-15
Damage from test 28*

Inverter Cabinet

Arc-flash experiments for a central inverter were performed on a mock-up assembly as shown in Figure 2-16 (right). The spacings between the bus bar and the cabinet were adapted from a Solectrica SGI 500XTM inverter to mock up an inverter cabinet. The cabinet included two sides and the top. Because the incoming supply was connected to the bottom of the busbars, the magnetic forces push the arc towards the top of the cabinet. Faults were triggered with a #30 copper wire.



Figure 2-16
Image of an inverter cabinet used as a reference (left) and the mocked-up assembly (right)

Ten experiments were performed at different irradiance and temperature with target duration of 2 secs of arc time. 1000 kW (nameplate capacity) of PV-array source was connected for all ten experiments. The inverter was turned on and connected in one of the experiments (#23) in order to observe the reverse feed from the inverter and/or grid in the event of arc-flash in the dc side. Table 2-3 shows the variables of arc-flash experiment on the mock inverter cabinet with irradiance and temperature data recorded during the experiments.

Table 2-3
Variables for inverter-cabinet experiments

Experiment No.	PV-array (dc-nameplate, kW)	Irradiance (W/m ²)	Temperature (Module °C)	Negative-Terminal grounded (Y/N)	Inverter Status (Switch On/Off)
21	1000	740	48	Y	OFF
22	1000	773	49	Y	OFF
23	1000	848	51	Y	ON
24	1000	830	54	Y	OFF
25	1000	850	55	Y	OFF
29	1000	780	54	Y	OFF
30	1000	810	54	N	OFF
31	1000	513	53	N	OFF
32	1000	970	59	N	OFF
33	1000	680	54	N	OFF

In the inverter cabinet, arcs were initiated in a variety of ways and in a variety of locations. Figure 2-17 shows the arc initiation for test 21, where a #30-Cu wire was used. In this test, the arc self-cleared in 0.13 secs. Figure 2-18 shows a test initiated with a wrench between the two busbars. In this test, the fault started as a nearly bolted fault. The arc voltage ramped up during the event, reaching 300 V by the end of the event. The damage from this event occurred at the busbar where the wrench was attached. Figure 2-19 shows a fault initiation for test 23. This event arced for the full duration of the test. The arc propagated to the top of the busbar and arced between the positive busbar and the case (see Figure 2-20). Test 24 was initiated similarly. In test 23, several strands in a braid were used to initiate the arc. The larger braid was used in tests 23, 24, 25, and 33. In these tests, the fault often started as a nearly bolted fault, and the braid burned clear after 0.25 to 0.5 secs. This reduced the overall arcing duration.

Figure 2-21 shows an arc initiated between the positive busbar and the equipment case in test 25. In this test, the arc moved to the top of the enclosure and continued to arc between the busbar and the equipment case.



*Figure 2-17
Arc initiation in the inverter cabinet for test 21*



*Figure 2-18
Arc initiation in the inverter cabinet for test 22*

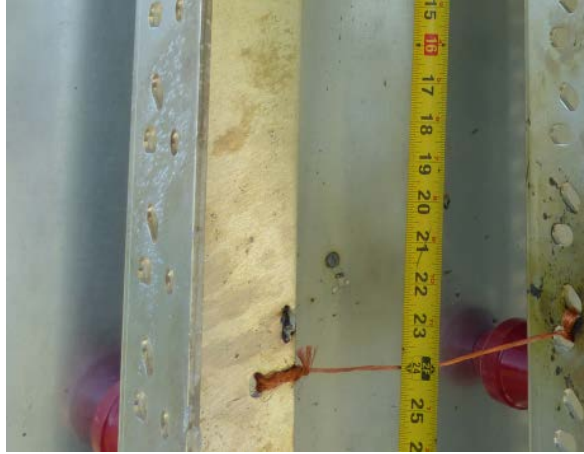


Figure 2-19
Arc initiation in the inverter cabinet for test 23



Figure 2-20
Arc damage from test 23



Figure 2-21
Arc initiation in the inverter cabinet for test 25

Figure 2-22 shows a fault initiated on another set of busbars with one-inch spacing. As with the inverter tests discussed above, the arc moved to the top of the positive busbar and arced to the equipment case. See the damage from this test in Figure 2-23. Figure 2-24 shows images before and during this test.



*Figure 2-22
Bus arrangement for test 29*



*Figure 2-23
Arc damage for test 29*

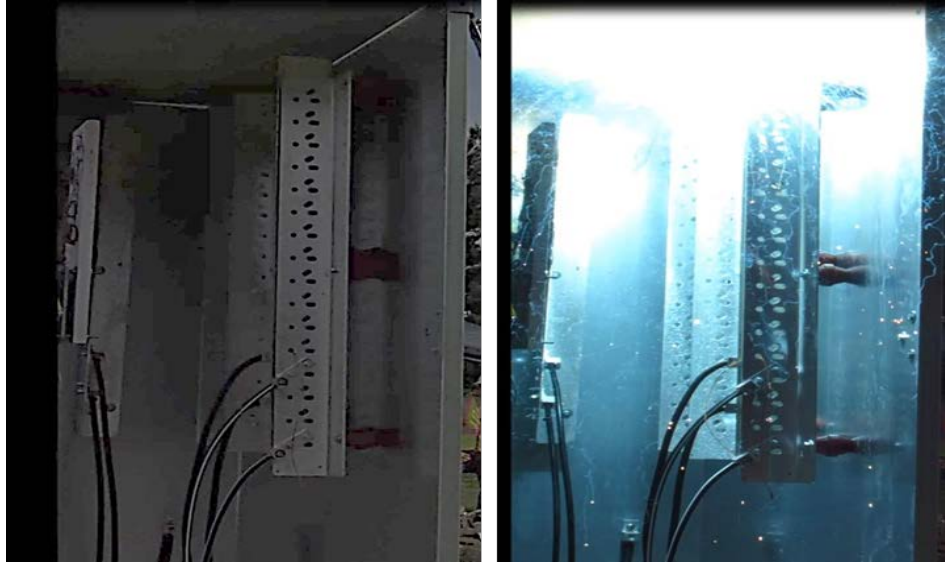


Figure 2-24
Inverter before and during test 29

Results Summary

Table 2-4 summarizes the results from each test. The “time” column is the duration that the source voltage was applied. Some of the events self-cleared, so in those events, fault current was not flowing for the entire time period.

Table 2-4
Summary of test results

Test	Source (kW)	Bus Spacing (in)	Irradiance (W/m ²)	Temp of Backsheet (°C)	Open-Circuit Voltage (V)	Time (s)	Current (A)	Voltage (V)	Power (kW)	Energy (kJ)	Maximum Incident Energy (cal/cm ²)	Notes
20-in box tests												
1	250	0.5	878	58		0.38	328	386	126.9	47.6	0.1	
2	250	0.5	780	46		0.40	318	353	112.1	44.9	0.0	3
3	1000	0.5	1000	51		1.90	1478	216	319.6	607.2	3.6	
4	500	0.5	830	46		1.88	697	234	163.1	305.7	1.4	2
5	500	0.5	725	47		1.88	427	267	114.1	214.0	0.6	
6	1000	2	665	52		1.88	986	322	317.3	594.9	2.1	
7	1000	2	640	50		1.63	951	105	100.2	162.8	0.3	
34	1000	2	810	49	758	1.90	1109	310	344.0	653.6	2.0	
35	1000	2	680	45		0.13	656	495	324.7	40.6	0.1	1, 5
36	125	2	667	49	779	7.68	128	231	29.5	226.3	0.8	
Inverter tests												
21	1000		740	48	772	0.13	622	394	244.9	30.6	0.4	5
22	1000		773	49	768	1.83	1175	146	171.4	312.8	0.7	4
23	1000		848	51	580	1.95	1388	141	195.3	380.7	0.6	2
24	1000		830	54	762	1.48	1269	207	202.6	374.8	0.6	6
25	1000		850	55	756	1.63	1220	201	201.7	378.2	0.6	6
29	1000		780	54	754	1.88	1223	159	195.0	365.6	0.8	
30	1000		810	54		0.35	1084	407	440.9	154.3	0.3	1, 5
31	1000		513	53		0.48	707	156	110.5	52.5	0.0	1, 5
32	1000		970	59		0.20	1137	371	422.1	84.4	0.2	1, 5
33	1000		680	54		1.28	1044	286	197.7	375.7	0.4	1, 6
Combiner-box tests												
26	1000		530	52	758	1.88	725	273	197.7	370.7	2.6	
27	1000		950	53	769	1.88	1408	224	315.4	591.3	2.6	
28	1000		970	58	757	9.90	1406	202	284.4	2816.0	11.7	

Notes:

1. The negative terminal was ungrounded (floating). Most tests had the negative terminal tied to the equipment ground.
2. Inverter was on. Most tests had the inverter off.
3. Combiner-box 2 on inverter A was found open; current dropped mid test.
4. Wrench used to initiate fault.
5. Fault self-cleared.
6. Fault duration was less than target because a larger braid was used to initiate the test (that took time to burn clear).

Section 3: Analysis of Results

Arc Current and Voltages

PV modules are a non-linear power source. Under normal operating conditions, their current is set by the incoming irradiance at any given time. The voltage set point is determined by the inverter, most often through maximum power point tracking (MPPT) algorithms. This testing provides data on the behavior of the current and voltage during an arcing fault with the PV array as the source. The voltage and current can be compared to the characteristic parameters of the PV array, including the short-circuit current (I_{sc}), the current at maximum power (I_{mp}), the open-circuit voltage (V_{oc}), and the voltage at maximum power (V_{mp}).

In all tests, the modules provided a constant current during the course of testing, in line with expectations from a constant irradiance over such a short time period. Figure 3-1 shows the current and voltage of a 1000-kW PV array, during an arc-flash. The constant-current characteristic is quite different than ac arc flash where the current is generally quite chaotic.

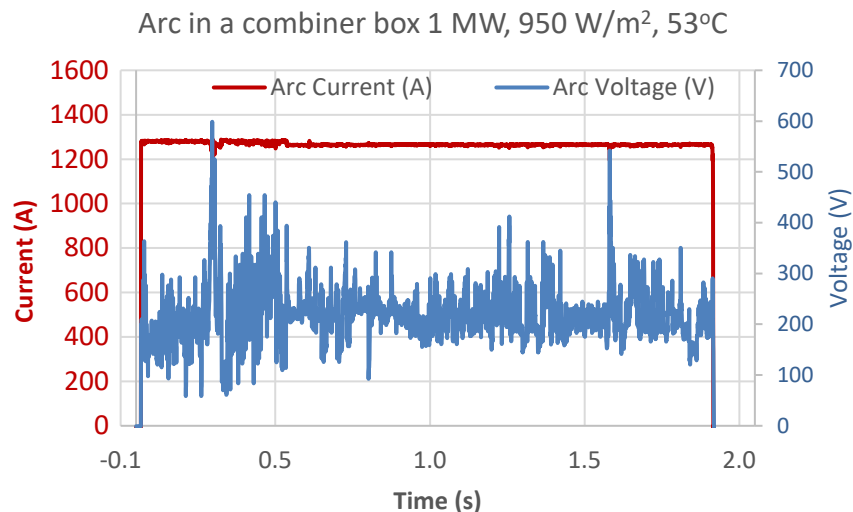


Figure 3-1

Arc current and voltage of a PV-array (1000 kW), 950 W/m² irradiances and 53°C PV-module temperature (Experiment no. 27; inverter switched-off)

The average current through the circuit and arc (I_{arc}) was higher than current at maximum power (I_{mp}) and close to the short-circuit current (I_{sc}) of the array. The ratio of I_{arc}/I_{mp} is plotted on Figure 3-2. There was no dependency on the testing assembly or the electrode gap. In contrast, the arc-voltage (V_{arc}) was less uniform throughout the tests as shown in Figure 3-1. On average, V_{arc} decreased to one quarter of the open-circuit voltage of the array (V_{oc}) and inverse correlates with the electrode gap in the test assembly. The ratio of arc-voltage to array voltage at maximum power (V_{mp}) is shown in Figure 3-2. The ratio V_{arc}/V_{mp} was consistent for each electrode gap (0.5 and 2.0 in; 1 and 5 cm) in the 20-in (51-cm) box and more variable for the inverter and combiner box tests due to variation on the location of arc initiation which alters the electrode gap and the propagation of the arc.

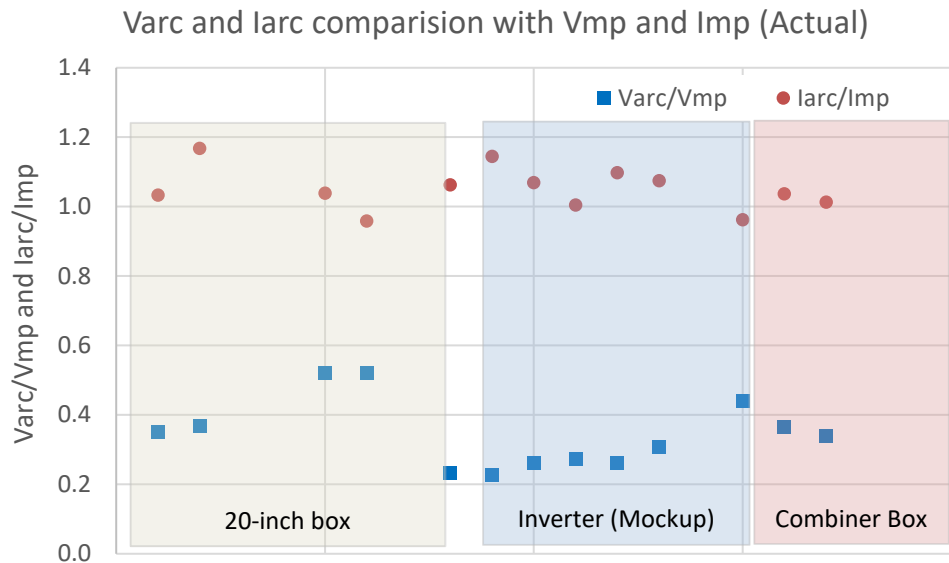


Figure 3-2
Ratios of V_{arc}/V_{mp} and I_{arc}/I_{mp}

For a given test, the arc current (I_{arc}) remained constant throughout the arcing phenomena, irrespective of electrode geometry and source size. The median value of I_{arc} was 104% of I_{mp} (actual) and consistent for all experiments. The arc voltage varied during the arcing phenomena as shown in Figure 3-1. The mean value of V_{arc} was dependent upon the geometry of arc-electrode assembly (spacing and shape) and the source size.

Electrode spacings of 0.5 and 2 in (1 and 5 cm) were used for the 20-in (51-cm) box tests. Several different gaps were included in the inverter tests. Arc voltage inversely correlated with electrode spacing. For the box tests with a 0.5-in (1-cm) spacing, V_{arc}/V_{mp} averaged 36% (V_{arc} averaged 225 V). For the box tests with a 2-in (5-cm) spacing, V_{arc}/V_{mp} averaged 52% (V_{arc} averaged 316 V).

Incident Energies and Arc Energies

The incident energy and arc energy were studied in more details using the 20-in (51-cm) box tests. Seven arc-flash experiments were performed with two for 250 kW, two for 500 kW, and three for 1000 kW PV-array size (name-plate capacity). Those experiments were performed at different solar irradiance, temperature, and arc duration. Average arc energies and incident energies for 250, 500, and 1000 kW of PV array is shown in Table 3-1. The 250-kW tests were done with a shorter duration. With 1000 kW connected, the arc energy was twice that with 500 kW connected.

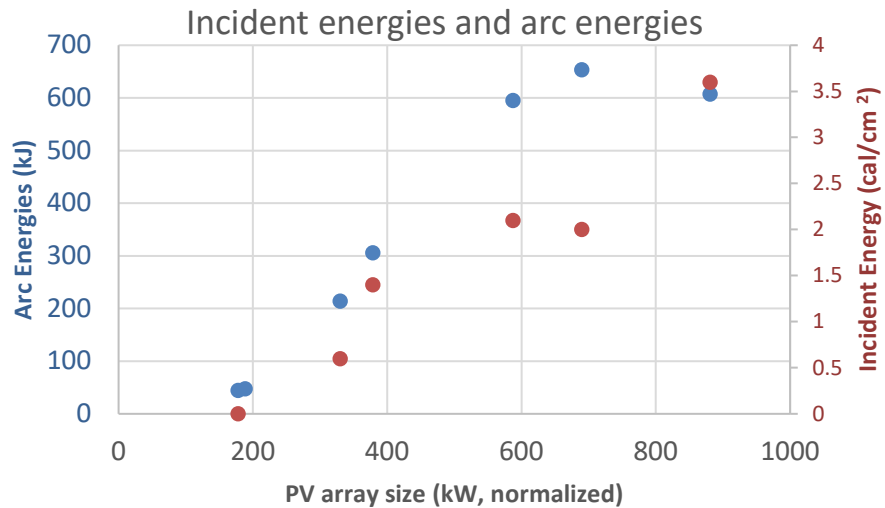


Figure 3-3
Incident and arc-flash energy as the function of PV array size

Measured incident energy shows a linear relation with PV-array size as depicted in Figure 3-3 with one outlier at the end (Exp.# 3). The distance between the electrodes was set at 0.5 in (1 cm) for experiment #3 in contrast to other experiments where the electrode gap was 2 in (5 cm). Smaller electrode gaps lead to a lower arc voltage, and that produces lower arc power and energy.

Table 3-1
Summary of results for the box experiments

Exp. No.	Source Size (kW)	Arc Duration (secs)	Solar Irradiance (W/m ²)	Incident Energy (cal/cm ²)	Arc Current (A)	Arc Voltage (V)	Arc Energy (kJ)
1	250	0.38	878	0.1	328	386	47.6
2	250	0.40	780	0.0	318	353	44.8
4	500	1.87	830	1.4	697	234	305.7
5	500	1.87	725	0.6	427	267	214.0
3	1000	1.87	1000	3.6	1,478	216	607.3
6	1000	1.87	665	2.1	986	322	594.9
34	1000	1.87	810	2.0	1,109	310	653.6

Incident energy correlated with arc energy. Figure 3-4 depicts a plots of arc energy against incident energy for all three setups, and Figure 3-5 depict the same for box tests with a gap of 0.5 in (1 cm).

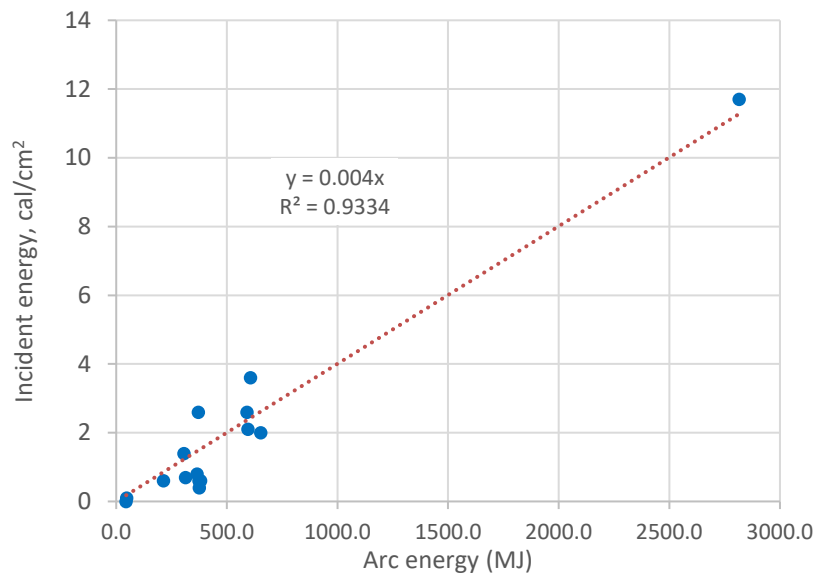


Figure 3-4
Arc energy (MJ) versus incident energy (cal/cm²) for all three experimental setups

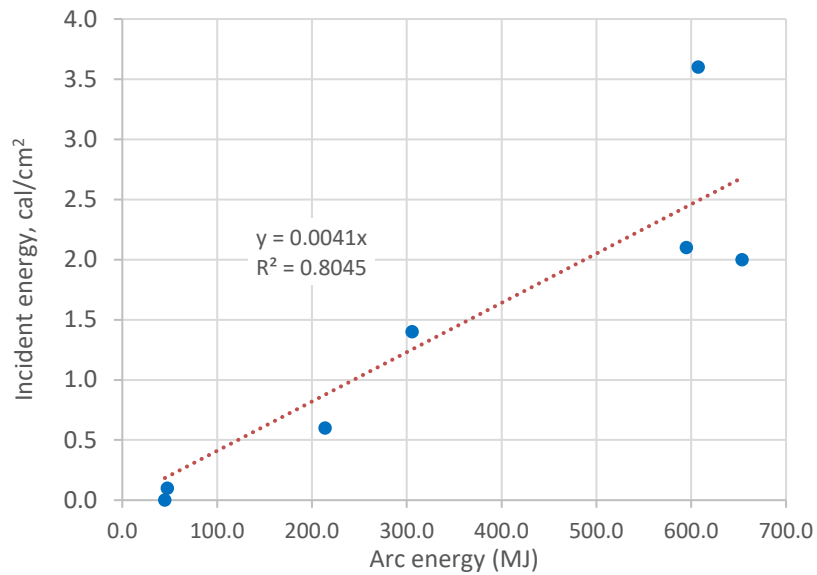


Figure 3-5
Arc energy (MJ) versus incident energy (cal/cm²) for the 20-in box setup

The amount of energy transmitted from the arc(s) to the calorimeters is comparable to similar tests for three-phase alternating current. Figure 3-6 shows the same data as Figure 3-5 with ac test results. These test data points are from IEEE/NFPA tests used for development of a new version of IEEE 1584 [11]. These tests have a 20×20×20-in (51×51×51-cm) box with three vertical electrodes. Both datasets have similar spread, and the multiplier factors are within 25% (4.1 vs. 5.4). One difference between the two tests is that the IEEE/NFPA tests were all less than 0.21 secs in duration with currents from 0.5 to 31 kA. The shorter, higher-magnitude events may have pushed more of the energy out of the enclosure and could explain why the energy transfer was somewhat higher for the ac tests.

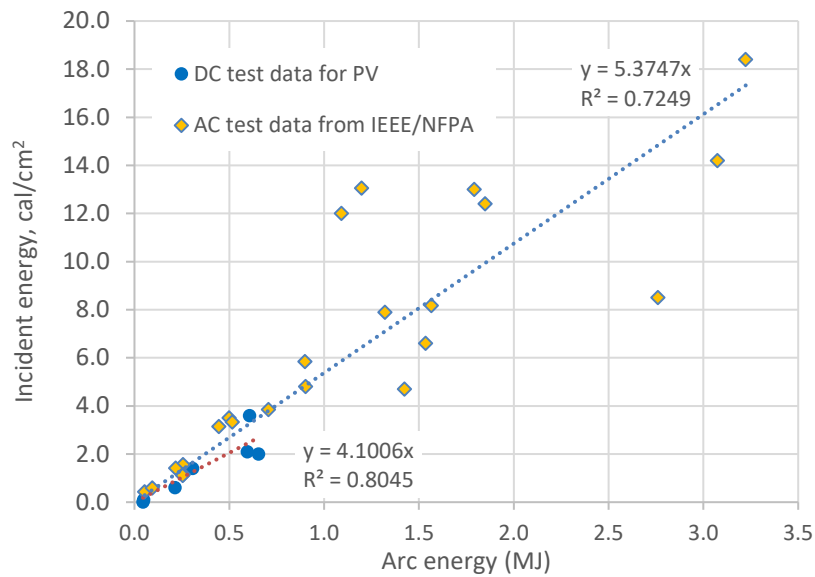


Figure 3-6
Comparison of energy transfers for ac and dc tests

Arc-Flash Duration Versus Arc Energy

Arc-flash energy shows a linear relation with arc durations with the same source and electrode geometry. Figure 3-7 shows the measured arc-flash energy for 0.5-, 2-, and 10-sec target durations (0.37-, 1.87-, and 9.90-sec actual duration).

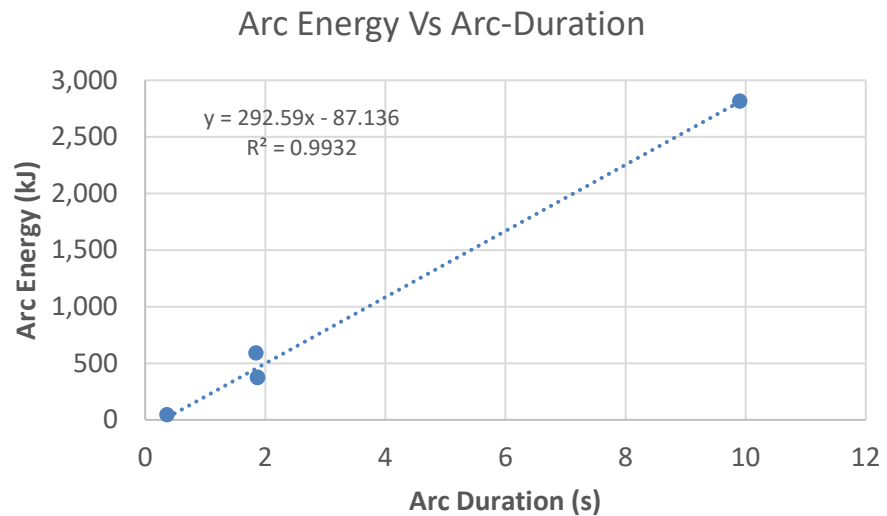


Figure 3-7
Measured arc-flash energy vs arc duration (box experiments)

Impact of the PV Source

A PV-array is a non-linear power source. This testing found that the arc-flash events operated near the short-circuit portion of the I - V curve. The measured values of I_{arc} and V_{arc} were compared with nameplate characteristics and with current and voltage that are adjusted for solar irradiance and temperature. Table 3-2 shows the current, voltage, and power of the PV array and measurements for an arc-flash test. The measured I_{arc} and V_{arc} are plotted along with the I - V -characteristic of the PV array in Figure 3-8. The PV array operates in a constant-current region of I - V -characteristic curve near the short-circuit end of the curve. Figure 3-9 shows the power-voltage characteristic of the same experiment and array conditions.

Table 3-2

Arc current, voltage, and power (I_{arc} , V_{arc} , and P_{arc}) of a PV-array during an arc flash in a PV inverter test (Test #27)

Parameters	Current (A)	Voltage (V)	Power (W)
Nameplate maximum power point	1,430	693	990,967
Adjusted maximum power point	1,358	612	830,439
Arc measurement, average	1,408	224	315,219
Arc measurement, median	1,438	222	318,666

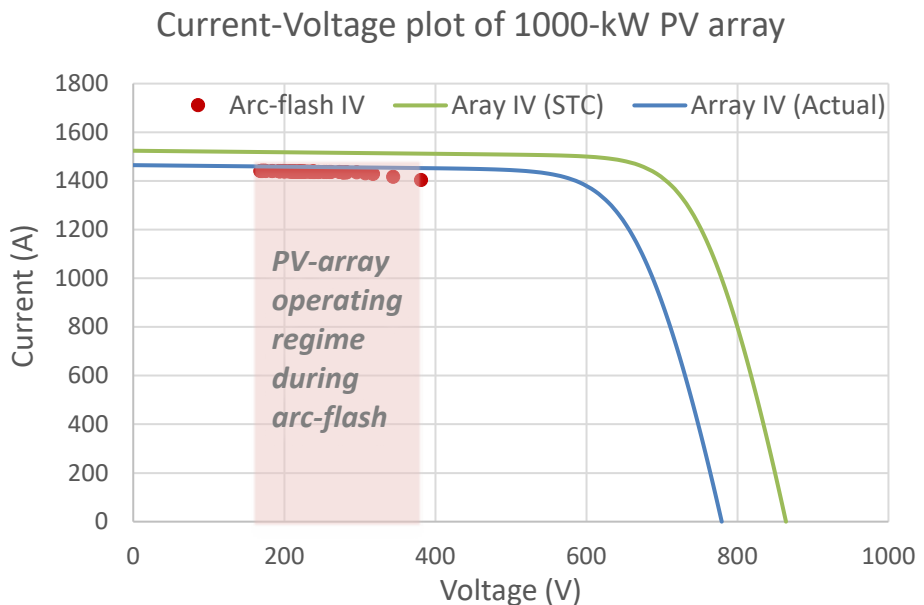


Figure 3-8

Arc current and voltage of a PV-array (1000kW), 950 Wm^{-2} irradiances and 53°C PV-module temperature (Experiment no. 27; an inverter switched-off)

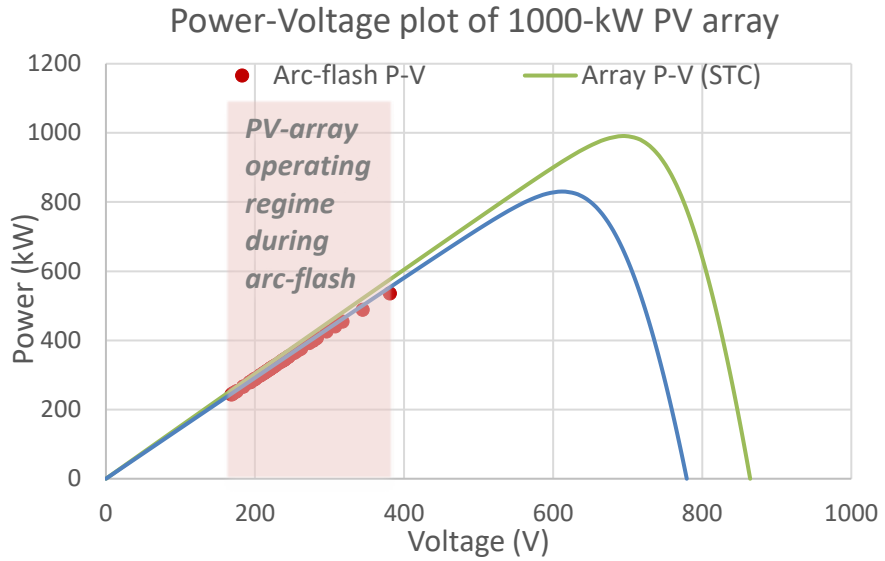


Figure 3-9
Power-Voltage characteristic of PV-array (~1000 kW, 950 W/m², 53°C module temperature).

Arc power (P_{arc}) was found to be dependent upon the test fixture assembly, especially with varying electrode gaps. The P_{arc}/P_{max} (actual) ratio for a 0.5-in (1-cm) electrode gap in the 20-in (51-cm) box was 0.36. For the combiner box, $P_{arc}/P_{max} = 0.38$.

Table 3-3
 P_{arc}/P_{max} for different test fixtures showing arc gap and connected array source size

Test	Test Fixture	Source kW	Electrode Spacing, in	P_{arc}/P_{max}
1	Box	250	0.5	0.67
2	Box	250	0.5	0.63
3	Box	1000	0.5	0.36
4	Box	500	0.5	0.43
5	Box	500	0.5	0.35
6	Box	1000	2	0.54
34	Box	1000	2	0.50
22	Inverter	1000		0.25
23	Inverter	1000		0.26
24	Inverter	1000		0.28
25	Inverter	1000		0.27
29	Inverter	1000		0.29

Table 3-3 (continued)

Parc/Pmax for different test fixtures showing arc gap and connected array source size

Test	Test Fixture	Source kW	Electrode Spacing, in	Parc/Pmax
33	Inverter	1000		0.33
26	Combiner box	1000		0.42
27	Combiner box	1000		0.38
28	Combiner box	1000		0.34

Effect of the Inverter Contribution

Arc flash on the dc side of a PV system can occur while the inverter is connected to a utility grid. Furthermore, discharge from the capacitors in the inverter can also feed the arc. Two arc-flash experiments were performed while the inverter was connected to observe the effect on arc flash.

The inverter caused a spike of current lasting approximately 50 msecs as shown in Figure 3-10, while no such spike was observed when the inverter was off as shown in Figure 3-1. Table 3-4 depicts the duration, current, voltage, and energy of the spike and the total energy for two experiments in the 20-in (51-cm) box (test #4) and the inverter mockup (test #23). The spike has resulted from the discharge of the capacitor and has approximately 12% of the total arc-flash energy.

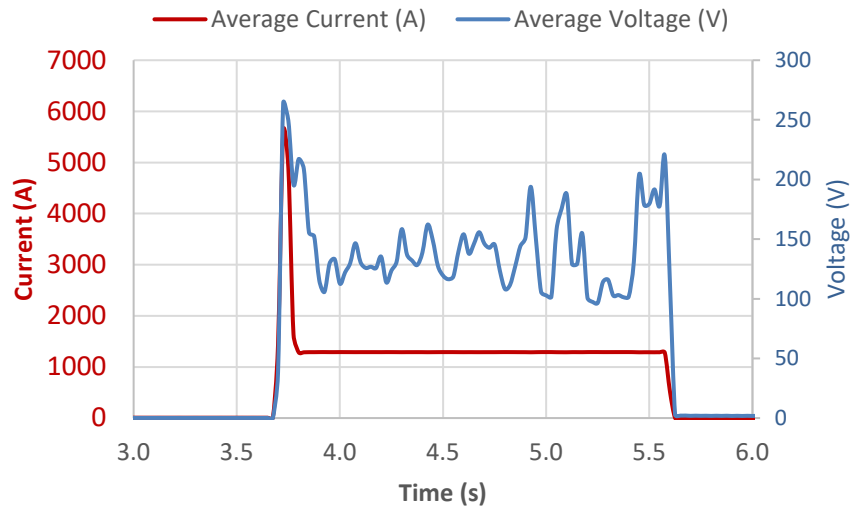


Figure 3-10
Average current and voltage during arc-flash with the inverter on

Table 3-4

Total and spike (due to the inverter) arc current, voltage, and energy of two experiments

Test number	Arc duration (secs)		Arc current (A)		Arc voltage (V)		Arc energy (kJ)	
	Total	Spike	Total	Spike	Total	Spike	Total	Spike
4	1.87	0.05	697	2537	234	352	306	45
23	1.90	0.05	1,388	3973	141	184	381	36

Directionality of the Arc Flash

Incident energies were measured by calorimeters in the sensor array. This had two main calorimeters, an upper unit and a lower unit. The directionality of the arc flash depended on the test assembly. For the 20-in (51-cm) box tests, the lower calorimeters measured higher incident energies. These had the supply fed from the top, and the arcs pushed towards the bottom of the box (Figure 3-11). In the 20-in (51-cm) box tests, the arc often flowed from the positive terminal to the negative terminal (the second and fourth panels in Figure 3-11). In some cases, the arc bridged the gap from the positive electrode to the bottom of the case as shown in the third panel in Figure 3-11. That corresponds to an arc length of more than 10 in (25 cm).

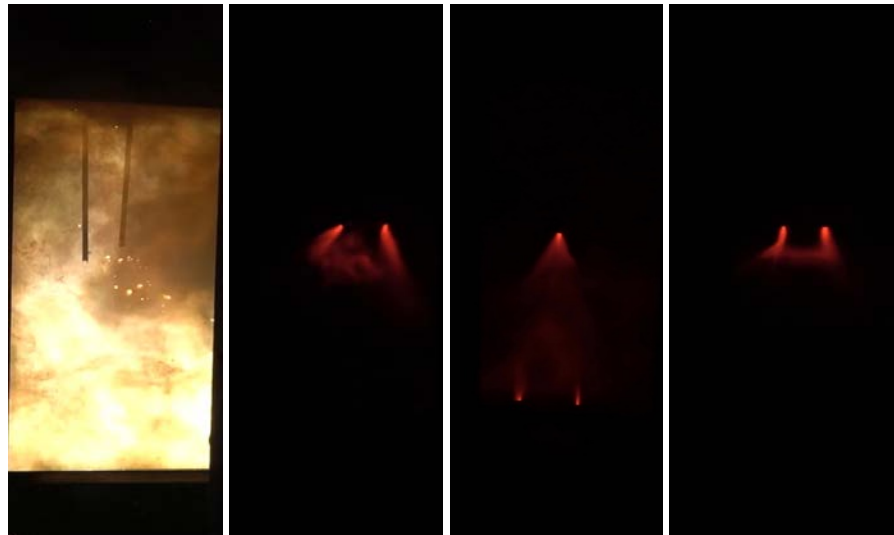


Figure 3-11
Arc flash and arc movement (infrared images) during test #34 in the 20-in (51-cm) box

In the combiner box tests and the inverter tests, the upper calorimeter measured higher incident energies. Both of these were fed from the bottom, and the forces pushed the arcs towards the top of the enclosure. Figure 3-12 and Figure 3-13 show arc flash movement in these enclosures.



Figure 3-12
Arc flash and arc movement (infrared images) during a test #28 in the combiner box



Figure 3-13
Arc flash and arc movement (infrared images) during a test #29 in the inverter assembly

Arc Stability and the Effect of Enclosure Grounding

Almost all of the tests had sustainable arcs. This differs from ac arc flash where it is common for arcs to self-extinguish if the system voltage is under 600 V [12, 6, 7]. In ac arc flash, the 60-Hz current will have a current zero every 8.3 msecs, and at each current zero, the current will extinguish. If the voltage across the arc is not sufficient to restrike the arc, the arc will stay extinguished. For the dc arcs in these tests, it is harder for faults to self-extinguish.

In test 21, the fault self-extinguished where a #30-Cu wire was used to initiate the fault across a gap of 7 in (Figure 2-17). Figure 3-14 shows the voltage and current during this test. The arc current began decreasing when the voltage reached about 70% of the open-circuit voltage. In other tests across this gap, a larger initiating wire was used, and that allowed enough extra heat and ionized copper to develop to sustain arcing. In real life, this is an unlikely fault initiation. It is likely that a tool will initiate the arc across a shorter distance.

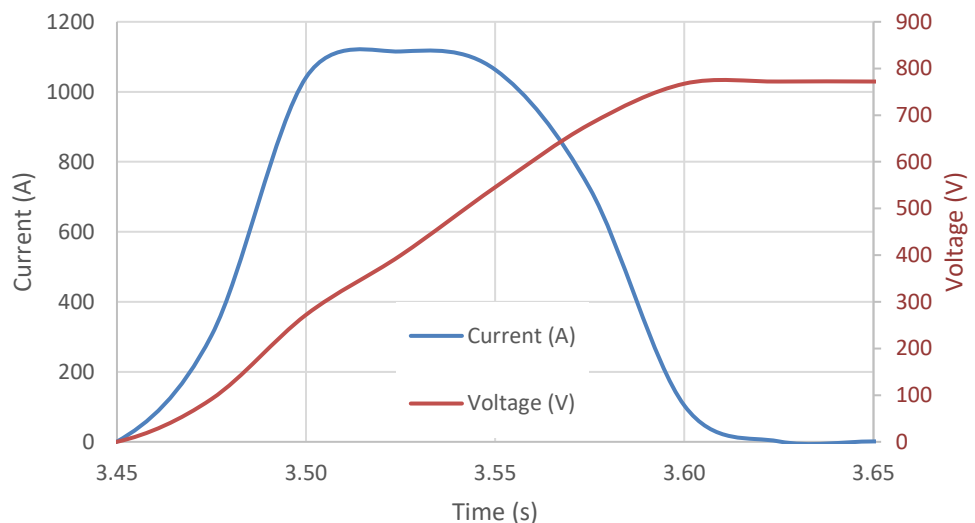


Figure 3-14
Arc voltage and current in test 21 that self-extinguished

Most of the tests were operated with the negative PV terminal connected to the equipment grounds. With this configuration, the equipment enclosure and equipment ground provide another path for return current. Five tests were operated with the negative terminal floated (one in the 20-in (51-cm) box and four in the inverter). All but one of these self-cleared before the dc contactor opened. Clearing times ranged from 0.13

to 0.48 secs. This suggests that it is much harder to sustain arcing if the arc cannot use the equipment ground as a return path. Without a return path through the equipment ground, the arc has to maintain a connection to the negative terminal, and the magnetic forces make that difficult.

Figure 3-15 shows all of the video frames for test 30 for a camera with an infrared-passing filter. This event self-cleared in approximately 0.25 secs. This test was in the inverter setup with a 1-in (2.5-cm) bus spacing (the location shown in Figure 2-22). Despite the tight bus spacing, the arc still self-extinguished. From Figure 3-15, it appears that the arc on the positive terminal on the left bowed away, and the arc became too long to sustain. The arc also appeared to be moving quickly.

Because arcs are more likely to self-clear if the negative terminal is floating, this highlights the benefit of having a protective device between the negative terminal and the local ground. When that operates, arcing faults will be more likely to self-clear because the equipment case and equipment grounds cannot provide a return path for current.

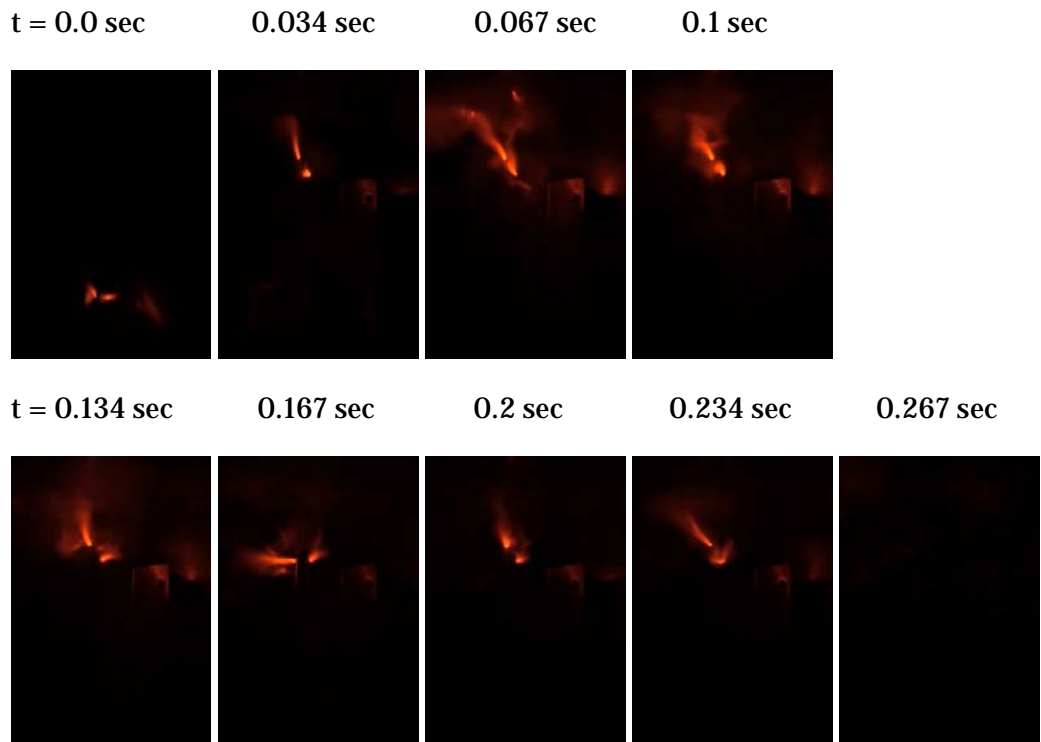


Figure 3-15
Infrared filtered video frames for test 30

Using Test Results to Determine Appropriate Protective Levels

One way to estimate the arc rating of clothing systems (in cal/cm²) required for workers is to use the test results. This is the approach used in the NESC [2], where a table is provided showing the required rating of clothing systems for various equipment for ac voltages from 50 V to 1000 V.

To use this data to determine the protective level needed for PV equipment, the test data can be normalized as follows:

- Arcing duration = 2 secs
- Irradiance = 1000 W/m²
- Array size = 1000 kW
- Array short-circuit current = 1500 A

Figure 3-16 shows a histogram of the maximum measured incident energies normalized to the parameters above. Figure 3-17 shows a cumulative distribution of the same data. These are incident energies at 18 in (46 cm). The maximum adjusted incident energy is 5.2 cal/cm² measured on the first test of the combiner box. Note that this data excludes events that self-cleared in less than 0.3 secs or had a maximum incident energy of zero.

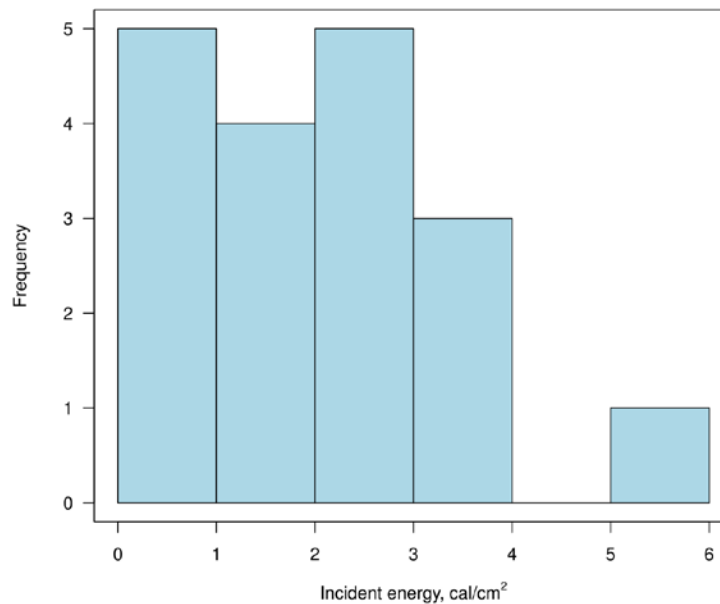


Figure 3-16
Histogram of adjusted incident energies

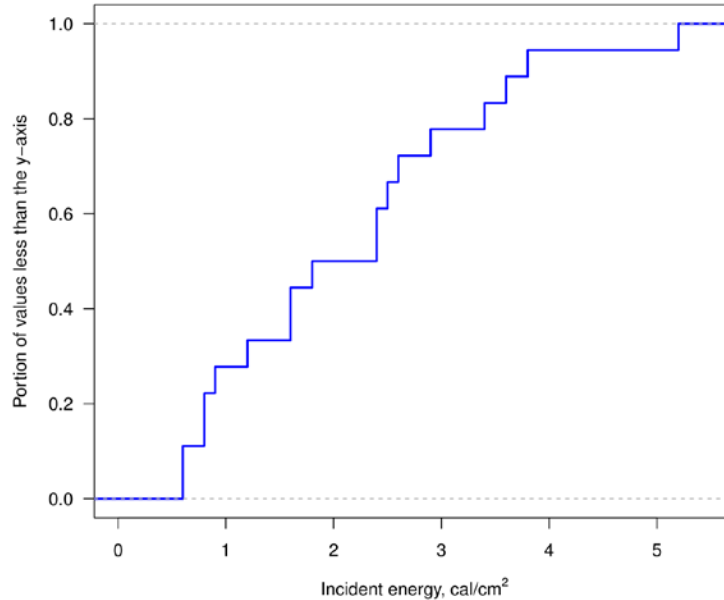


Figure 3-17
Cumulative distribution of adjusted incident energies

With the incident energy measurements scaled to the same inputs, the adjusted incident energies should all be similar. There is some spread in the results due to the differences in transfer of energy from the arc to the measurement point. Table 3-5 shows the adjusted incident energies for each of the tests. The adjusted incident energies varied by configuration:

- 20-in box tests → average = 2.6 cal/cm²; median = 2.6 cal/cm²
- Inverter tests → average = 1.1 cal/cm²; median = 0.9 cal/cm²
- Combiner-box tests → average = 3.5 cal/cm²; median = 2.9 cal/cm²

The tests in the inverter cabinet had lower adjusted incident energies. In the inverter cabinet, the calorimeters were less likely to be at the location where the incident energy was highest. The arcs had much more room for movement in the inverter cabinet. This spread out the location of the arc energy and distributed the incident energy across a broader area.

The maximum adjusted incident energy of 5.2 cal/cm² is a good starting point for determining clothing requirements. With the assumptions of a 2-sec duration, an 18-in (46-cm) working distance, and an array source of 1000 kW (with a short-circuit current of 1500 A), incident energies should be less than 5.2 cal/cm². Adding a safety margin, it should be sufficient to protect workers with 8 cal/cm² clothing systems.

For other array sizes or event durations, the results could be linearly scaled. For a 1500-kW system with a short-circuit current of 2250 A, the maximum adjusted incident energy would be $1.5 \times 5.2 = 7.8$ cal/cm², so clothing could be selected based on that.

Table 3-5
Adjusted incident energies

Test	Source (kW)	Irradiance (W/m ²)	Time (s)	Maximum Incident Energy (cal/cm ²)	Adjusted Maximum Incident Energy (cal/cm ²)
20-in box tests					
1	250	878	0.38	0.1	2.4
2	250	780	0.40	0.0	
3	1000	1000	1.90	3.6	3.8
4	500	830	1.88	1.4	3.6
5	500	725	1.88	0.6	1.8
6	1000	665	1.88	2.1	3.4
7	1000	640	1.63	0.3	0.6
34	1000	810	1.90	2.0	2.6
35	1000	680	0.13	0.1	
36	125	667	7.68	0.8	2.5
Inverter tests					
21	1000	740	0.13	0.4	
22	1000	773	1.83	0.7	1.2
23	1000	848	1.95	0.6	0.9
24	1000	830	1.48	0.6	0.8
25	1000	850	1.63	0.6	0.8
29	1000	780	1.88	0.8	1.6
30	1000	810	0.35	0.3	1.6
31	1000	513	0.48	0.0	
32	1000	970	0.20	0.2	
33	1000	680	1.28	0.4	0.6
Combiner-box tests					
26	1000	530	1.88	2.6	5.2
27	1000	950	1.88	2.6	2.9
28	1000	970	9.90	11.7	2.4



Section 4: Models of Arc Flash in PV Systems

Industry Models

A number of industry models are available to estimate incident energies for dc arc flash. The calculation approaches considered in this section are based on a consolidated approach [13] and spreadsheet [14] developed by the DC Arc Flash Working Group of the EFCOG. The models included in that spreadsheet plus others are compared to the test results.

Measured incident energies (IE) from a sampling of the experiments in the 20-in (51-cm) box are compared against the calculated incident energies using common dc arc-flash calculation models [15, 4, 16, 17]. Inputs to the models were the actual open-circuit voltage and short-circuit current of the PV array during for each test. Each test was corrected for plane-of-array irradiance and temperature. A uniform irradiance and a uniform temperature profile across the array were assumed.

Table 4-1 shows the measured incident energies and corresponding predictions from several models for those tests. The dc power of the PV array that's shown is corrected for irradiance and temperature during each test. The Doan and the Enrique et al. models are more than five times the measured incident energies. The Paukert and the Stokes and Oppenlander models match closely for the configurations with a 0.5-in (1-cm) spacing, but for the tests with a 2-in (5-cm) spacing, the predictions are about twice that measured.

Table 4-1

Measured incident energy and calculated incident energies using different models

Test	PV-array (at STC) (kW)	Spacing (in)	Measured Incident Energy (cal/cm ²)	Incident Energies from Models (cal/cm ²)			
				Paukert [17]	Stokes & Oppen. [15, 17]	Doan [4]	Enrique et al. [16]
2	178 (250)	0.5	0.0	0.10	0.12	0.48	1.44
4	378 (500)	0.5	1.4	1.15	1.36	5.10	13.91
5	329 (500)	0.5	0.6	0.99	1.17	4.41	12.06
3	881 (1000)	0.5	3.6	3.17	3.59	12.12	31.64
6	587 (1000)	2.0	2.1	3.69	3.76	7.88	20.98
34	690 (1000)	2.0	2.0	4.65	4.67	9.45	25.01

All of the models in Table 4-1 have a similar format using the approach from EFCOG [13, 14]. The incident energies are based on:

$$E = (V_{arc} \cdot I_{arc} \cdot T) \cdot 0.239 \cdot \frac{1}{4\pi \cdot D^2} \cdot k_b$$

Where:

E = incident energy, cal/cm²

V_{arc} = arc voltage, V

I_{arc} = arc current, A

T = fault duration, secs

D = distance to the arc source, cm

k_b = configuration-correction factor

In this equation, the first term in parenthesis is the arc energy. The 0.239 factor converts joules to calories. The fraction $1/(4\pi \cdot D^2)$ is the ideal energy transfer from a point source of energy to the surface of a sphere at a distance D .

The factor k_b is a configuration-correction factor to account for focusing effects for arcs in equipment. This is based on the analysis of Wilkins et al. [18]. For an arc in open air, $k_b = 1$. For large switchgear, medium switchgear, and small panel, this factor is 1, 2.2, and 1.52 respectively. For the 20-in (51-cm) box tests shown in Table 4-1, the assumptions for low-voltage switchgear were used where $R_{EFF} = 640.0$ mm, $a = 400$ mm, and $k = 0.312$.

The main differences in each of the models is the assumptions each uses for V_{arc} and I_{arc} :

- *Doan*—This model assumes maximum power transfers to the arc with a linear source. $V_{arc} = V_{oc}/2$ and $I_{arc} = I_{sc}/2$.
- *Enrique et al.*—This model is tailored to PV systems and assumes that the maximum array power transfers to the arc. The voltage and current are both at the maximum-power point. $V_{arc} = V_{mp}$ and $I_{arc} = I_{mp}$.
- *Stokes and Oppenlander*—This model assumes that the arc has a nonlinear resistance based on z_g , the distance between electrodes in millimeters. V_{arc} and I_{arc} are found iteratively based on R_{arc} .

$$R_{arc} = \frac{20 + 0.534z_g}{I_{arc}^{0.88}}$$

- *Paukert et al.*—This model also assumes the arc has a nonlinear resistance. The resistance of the arc is based on a table of nonlinear functions for several electrode gaps.

Table 4-2 and Table 4-3 compare measured arc voltages and currents to predictions from models. None of the models compare well for either arc current or arc voltage. The Paukert et al. and Stokes and Oppenlander models both predict much small arc voltages than were measured. Both of these model the arc as a straight line from one electrode to another. In the tests, the arcs moved and stretched to much longer lengths. The maximum-power methods (Doan and Enrique et al.) both overpredict arc voltages. Arc currents match better.

Table 4-2
Measured arc voltage and calculated arc voltages using different models

Test	PV-array (at STC) (kW)	Spacing (in)	Measured arc voltage (V)	Arc Voltages from Models (V)			
				Paukert [17]	Stokes & Oppen. [15, 17]	Doan [4]	Enrique et al. [16]
2	178 (250)	0.5	353	42.4	53.4	396.6	635.5
4	378 (500)	0.5	234	47.9	57.8	397.7	634.6
5	329 (500)	0.5	267	46.9	57.3	393.7	633.4
3	881 (1000)	0.5	216	55.2	64.1	393.6	616.2
6	587 (1000)	2.0	322	105.7	107.8	384.5	618.9
34	690 (1000)	2.0	310	109.7	110.3	377.5	596.4

Table 4-3

Measured arc current and calculated arc currents using different models

Test	PV-array (at STC) (kW)	Spacing (in)	Measured arc current (A)	Arc Currents from Models (A)			
				Paukert [17]	Stokes & Oppen. [15, 17]	Doan [4]	Enrique et al. [16]
2	178 (250)	0.5	318	285.8	281.3	150.8	280.3
4	378 (500)	0.5	697	603.3	595.2	320.9	596.8
5	329 (500)	0.5	427	527.6	520.0	280.4	520.6
3	881 (1000)	0.5	1478	1432.9	1415.3	770.4	1429.9
6	587 (1000)	2.0	986	884.1	881.4	512.5	948.8
34	690 (1000)	2.0	1109	1070.1	1069.2	626.1	1156.8

Given that the Paukert and the Stokes and Oppenlander models badly underestimate the arc voltages (and thus the arc energies), why do they match measurements well? The answer appears to be due to the assumptions these models all use for energy transfer, including the configuration-correction factor.

The incident energy as a function of arc energy in these models is:

$$E = E_{arc} \cdot 0.239 \cdot \frac{1}{4\pi \cdot D^2} \cdot k_b$$

Where:

E = incident energy, cal/cm²

E_{arc} = arc energy, joules

D = distance to the arc source, cm

k_b = configuration-correction factor

With $D = 45.7$ cm (18 in) and $k_b = 2.2$, this becomes:

$$E = 20 \cdot 10^{-6} \cdot E_{arc}$$

The incident energy in cal/cm² is 20 times the arc energy in megajoules. In the measurements, the incident energy in cal/cm² was 4 times the arc energy in megajoules. See Figure 3-4. The factor of five difference between these values is the main reason that the Paukert and the Stokes and Oppenlander models compare reasonably well despite poorly predicting arc voltages. Several factors could explain why the measurements show less energy transfer from the arc than the theoretical model:

- Some of the arc energy acts to vaporize the electrodes. This energy may not transfer to the calorimeters.
- The box may absorb an appreciable portion of the arc energy.
- The arc moves, and that dynamically changes the distance to the calorimeters. There is no one fixed distance to the arc. Overall, this effect may reduce incident energies.
- The calorimeters may not always be positioned to capture the maximum incident energy.
- The configuration-correction factor may not be appropriate at a working distance as close as 18 in (46 cm). Likewise, the squaring term on the working distance may not be appropriate at a distance this close.

Given these factors, it is likely that the factor from measurements is more realistic than the factor assumed by these models.

New Model Based on Tests

In this section, a PV-focused model is considered that will more realistically capture the arc voltage, the arc current, and the incident energies. This is an empirical model based on the test results. This is similar to the approach used for the development of the model used in IEEE 1584 [1].

Consider the following model form:

$$E = (V_{arc} \cdot I_{arc} \cdot T) \cdot k_x$$

Where:

$$E = \text{incident energy, cal/cm}^2$$

$$V_{arc} = \text{arc voltage, V}$$

$$I_{arc} = \text{arc current, A}$$

$$T = \text{fault duration, secs}$$

$$k_x = \text{factor converting arc energy to incident energy at 18 in (46 cm), cal/cm}^2/\text{J}$$

Based on the test results, the following are appropriate values:

$$V_{arc} = 300 \text{ V}$$

$$I_{arc} = I_{sc} = \text{short-circuit current, A}$$

$$k_x = 4 \times 10^{-6} \text{ cal/cm}^2/\text{J}$$

With these values, the model becomes:

$$E = 0.0012 \cdot I_{sc} \cdot T$$

This model only applies for a working distance of 18 in (46 cm). For other working distance, a distance factor could be introduced as follows:

$$E = 0.0012 \cdot I_{sc} \cdot T \cdot \left(\frac{D}{45.7} \right)^{k_d}$$

Where

$$k_d = \text{distance coefficient} = -1.6$$

$$D = \text{distance to the arc source, cm}$$

For arc-in-a-box scenarios, the value of $k_d = -1.6$ was selected because the new draft version of IEEE 1584 [19] uses this factor for the distance coefficient for low-voltage ac equipment based on tests in a 20-in (51-in) box. Note that this is different than the factor of -2 used in the theoretical models.

The key factor in this model is the assumption of a constant arc voltage of 300 V. For an array with an open-circuit above 800 V, the 300 V is low enough to draw nearly the open-circuit current from the array. The arc voltage is determined primarily by the length of the arc, and the natural length of the arc is determined mainly by the geometry of the electrodes and the equipment. The 300 V is taken from the distribution of test data for arc voltages. The average arc voltage is reasonably consistent even in different scenarios tested.

Table 4-4 compares predictions from this model to the selected measurements compared above. All of the quantities compare well.

Table 4-4

Comparison of measurements to predictions from the empirical model

Test	PV-array (at STC) (kW)	Incident Energy (cal/cm ²)		Arc voltage (V)		Arc current (A)	
		Measured	Predicted	Measured	Predicted	Measured	Predicted
2	178 (250)	0.0	0.1	353	300	318	301.6
4	378 (500)	1.4	1.4	234	300	697	641.8
5	329 (500)	0.6	1.3	267	300	427	560.9
3	881 (1000)	3.6	3.5	216	300	1478	1540.7
6	587 (1000)	2.1	2.3	322	300	986	1025.0
34	690 (1000)	2.0	2.8	310	300	1109	1252.1

Section 5: Summary and Future Work

Key Findings

These tests provided a number of useful findings:

- Incident energy exposures to workers are modest, assuming a worker can self-extract in a reasonable time (2 secs for example). All incident energy measurements at a distance of 18 in (46 cm) to the equipment electrodes were less than 3.6 cal/cm². Extrapolating all tests to the highest irradiance and to a 2-sec duration produces a maximum adjusted incident energy of 5.2 cal/cm². Daily wear clothing of 8 cal/cm² should be sufficient for most equipment and PV array sizes.
- The nonlinear characteristics of PV panels are important to include. The PV array acts as a constant-current supply with currents near the short-circuit portion of the I-V curve of the array. The median arc voltage in tests was 234 V which was approximately 30% of the open-circuit voltage.
- The measured incident energies are lower than most of the industry models. Two of the industry models predicted over five times the energies measured. These “maximum-power” methods overpredicted energies. The Stokes and Oppenlander (1991) model provided results that were reasonable for an electrode gap of 0.5 in (1 cm). For a gap of 2 in (5 cm), the Stokes and Oppenlander model overpredicted incident energies by a factor of two. None of the models adequately predict incident energies across gap sizes. None of the models adequately predict arc currents and arc voltages.
- A custom model was developed to estimate incident energies on PV systems. The model predicts incident energy as a linear function of the short-circuit current of the array and the fault duration.
- Incident energies were comparable to ac arc flash when comparing normalized arc energies.
- Arcs sustained in many of the tests, and arcs also self-cleared in some tests. The open-circuit dc bus voltage was nominally 1000 V. During tests, the open-circuit array voltage was approximately 750 V. This voltage sustained arcs between gaps as long as 10 in (25 cm). With longer gaps, arcs were more likely to self-clear. None of the arcs self-cleared in the combiner box where the gaps between electrodes were less than 2 in (5 cm).

- If the inverter was on, there was minimal feed from the inverter to the arc. The main source of energy is still the PV array.
- The grounding and connection of the negative terminal is an important consideration. If the negative terminal is floating, an arc is less likely to sustain because the equipment case cannot act as a return path for the current. This is particularly important in the inverter cabinet where spacings are wide. In the inverter cabinet, limiting the sustainable faults to those that go from one bus to another bus greatly reduces the risks of sustainable faults.

Future Work

Future work is possible for better analysis of dc arc flash at photovoltaic installations:

- Tests at photovoltaic sites with 1500-V dc buses
- Better software models of dc arc flash
- Combined incident energies when there are ac and dc sources in the same area (as in the inverter)
- Tests in more geometries
- Share results with the industry and standards bodies

Future work could also include sharing results with the industry and standards bodies. This will provide more opportunities for feedback and help inform operations and maintenance practices at photovoltaic sites.


Related work could also follow for other dc applications, like dc energy storage sites or dc fast charging sites. Because the results in this report showed the importance of the source characteristics, this follow-up work could include tests with batteries and other devices included at these types of sites.



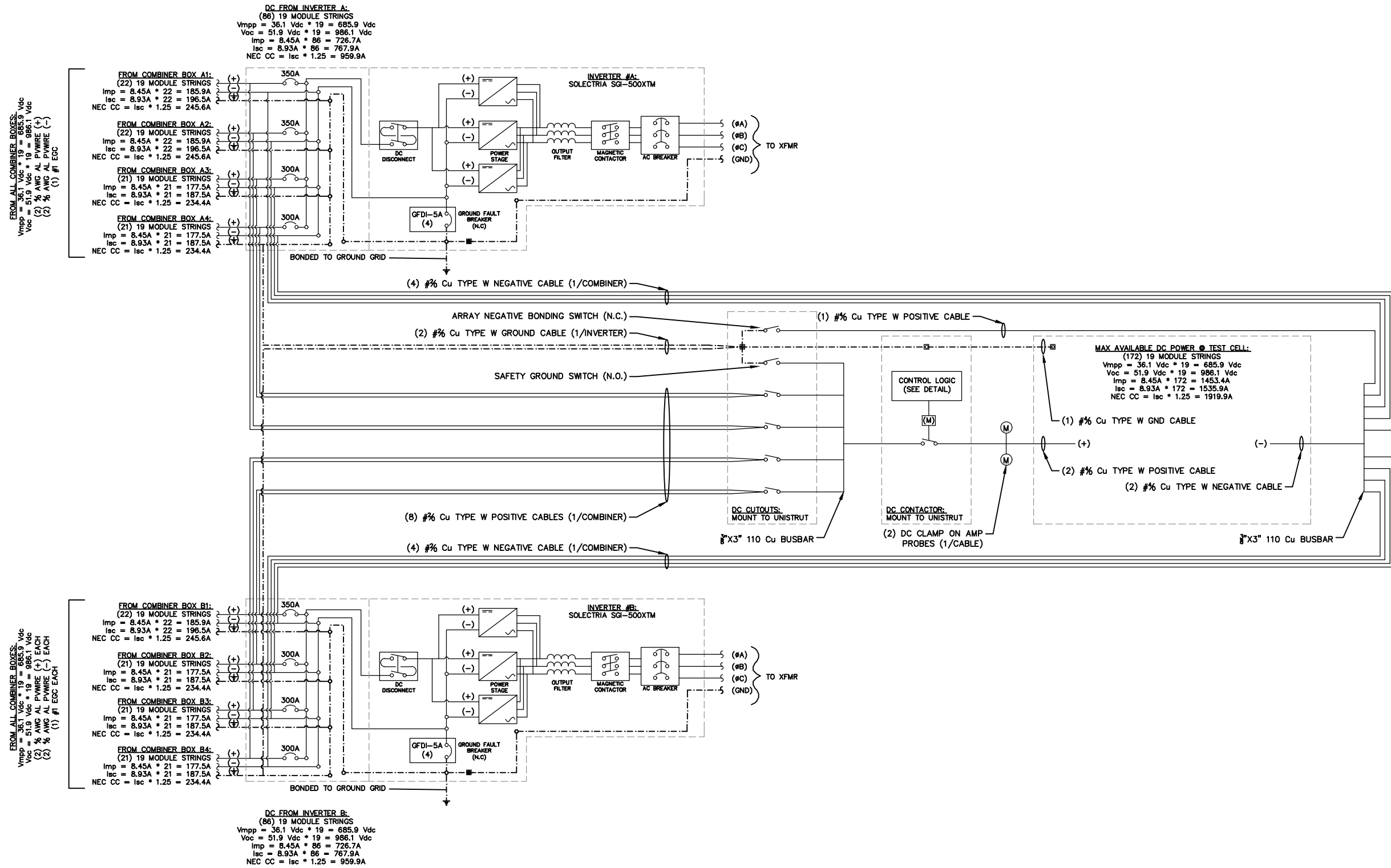
Section 6: References

1. IEEE Std. 1584-2002, IEEE Guide for Performing Arc Flash Hazard Calculations.
2. IEEE C2-2017, National Electrical Safety Code, 2017.
3. NFPA 70E, Standard for Electrical Safety in the Workplace, National Fire Protection Association, 2018.
4. D. R. Doan, "Arc Flash Calculations for Exposures to DC Systems," IEEE Transactions on Industry Applications, vol. 46, no. 6, pp. 2299 - 2302, 2010.
5. *Distribution Arc Flash: Analysis Methods and Arc Characteristics*. EPRI, Palo Alto, CA: 2009. 1018693.
6. *480-V Distribution Arc Flash Updates*. EPRI, Palo Alto, CA: 2011. 1022002.
7. *Arc Flash Update for 480-V Network Protectors*. EPRI, Palo Alto, CA: 2015. 3002006373.
8. *Medium-Voltage Arc Flash: Switchgear and Live-Front Transformers*. EPRI, Palo Alto, CA: 2015. 3002005598.
9. ASTM F1959 / F1959M-14e1, Standard Test Method for Determining the Arc Rating of Materials for Clothing, vol. 14e1, West Conshohocken, PA: ASTM International, 2014.
10. J. Potvin, Method for Measuring the Individual Incident Energy Contributors during an Arc Flash Event, PhD dissertation, Clarkson University, 2018.
11. W.-J. Lee, T. Gammon, Z. Zhang, B. Johnson and S. Vogel, "IEEE/NFPA Collaboration on Arc Flash Phenomena Research Project," Power and Energy Magazine, pp. 116-123, Oct. 2012.
12. *208-V Arc Flash Testing: Network Protectors and Meters*. EPRI, Palo Alto, CA: 2010. 1022218.
13. DC Arc Flash Working Group, Best Practice: Calculation Spreadsheet for DC Arc Flash Hazard, EFCOG, 2016.
14. DC Arc Flash Working Group, DC Arc Flash Calculator, EFCOG, 2018.
15. A. D. Stokes and W. T. Oppenlander, "Electric arcs in open air," Journal of Physics D: Applied Physics, vol. 24, no. 1, pp. 26-35, 1991.

16. E. H. Enrique, P. N. Haub and T. P. Bailey, "DC arc flash calculations for solar farms," in 1st IEEE Conference on Technologies for Sustainability (SusTech), Portland, OR, 2013.
17. R. F. Ammerman, T. Gammon, P. K. Sen and J. P. Nelson, "DC-Arc Models and Incident-Energy Calculations," IEEE Transactions on Industry Applications, vol. 46, no. 5, 2010.
18. R. Wilkins, M. Allison and M. Lang, "Improved method for arc flash hazard analysis," in Industrial and Commercial Power Systems Technical Conference, Florida, 2004.
19. P1584/D4, Draft Guide for Performing Arc-Flash Hazard Calculations, IEEE Arc Flash Hazard Calculations Working Group, 2018.



Appendix A: Three-Line Diagram of the Test Setup



		INDUSTRIA ENGINEERING, INC. 1 ASH STREET HOPKINTON, MA 01748	
TITLE EPRI THREE-LINE DIAGRAM			
PROJECT NGRID/EPRI Arc Flash Testing			
SITE Kelly rd. Sturbridge, MA			
CLIENT National Grid			
DESIGNED	CHECKED	FILENAME	DATE
GM	--		AUG 2017
			FIGURE

Export Control Restrictions

Access to and use of EPRI Intellectual Property is granted with the specific understanding and requirement that responsibility for ensuring full compliance with all applicable U.S. and foreign export laws and regulations is being undertaken by you and your company. This includes an obligation to ensure that any individual receiving access hereunder who is not a U.S. citizen or permanent U.S. resident is permitted access under applicable U.S. and foreign export laws and regulations. In the event you are uncertain whether you or your company may lawfully obtain access to this EPRI Intellectual Property, you acknowledge that it is your obligation to consult with your company's legal counsel to determine whether this access is lawful. Although EPRI may make available on a case-by-case basis an informal assessment of the applicable U.S. export classification for specific EPRI Intellectual Property, you and your company acknowledge that this assessment is solely for informational purposes and not for reliance purposes. You and your company acknowledge that it is still the obligation of you and your company to make your own assessment of the applicable U.S. export classification and ensure compliance accordingly. You and your company understand and acknowledge your obligations to make a prompt report to EPRI and the appropriate authorities regarding any access to or use of EPRI Intellectual Property hereunder that may be in violation of applicable U.S. or foreign export laws or regulations.

The Electric Power Research Institute Inc., (EPRI, www.epri.com) conducts research and development relating to the generation, delivery and use of electricity for the benefit of the public. An independent, nonprofit organization, EPRI brings together its scientists and engineers as well as experts from academia and industry to help address challenges in electricity, including reliability, efficiency, affordability, health, safety and the environment. EPRI members represent 90% of the electric utility revenue in the United States with international participation in 35 countries. EPRI's principal offices and laboratories are located in Palo Alto, Calif.; Charlotte, N.C.; Knoxville, Tenn.; and Lenox, Mass.

Together...Shaping the Future of Electricity

Program:

Distribution Systems

© 2018 Electric Power Research Institute (EPRI), Inc. All rights reserved. Electric Power Research Institute, EPRI, and TOGETHER...SHAPING THE FUTURE OF ELECTRICITY are registered service marks of the Electric Power Research Institute, Inc.

3002011092

Electric Power Research Institute

3420 Hillview Avenue, Palo Alto, California 94304-1338 • PO Box 10412, Palo Alto, California 94303-0813 USA
800.313.3774 • 650.855.2121 • askepri@epri.com • www.epri.com